NOTIONAL SYSTEM MODELS

Technical Report

Submitted to:
The Office of Naval Research

Contract Number: N0014-08-1-0080

Submitted by:
Mike Andrus, Florida State University
Matthew Bosworth, Florida State University
Jonathan Crider, Purdue University
Hamid Ouroua, University of Texas at Austin
Enrico Santi, University of South Carolina
Scott Sudhoff, Purdue University

December, 2013

ELECTRIC SHIP RESEARCH
ESRDC
AND DEVELOPMENT CONSORTIUM

MISSION STATEMENT

The Electric Ship Research and Development Consortium brings together in a single entity the combined programs and resources of leading electric power research institutions to advance near- to mid-term electric ship concepts. The consortium is supported through a grant from the United States Office of Naval Research.

FLORIDA STATE UNIVERSITY · 1851

Massachusetts Institute of Technology

MISSISSIPPI STATE UNIVERSITY

NPS PRAESTANTIA PER SCIENTIAM 1909 — NAVAL POSTGRADUATE SCHOOL

PURDUE UNIVERSITY

UNIVERSITY OF SOUTH CAROLINA

THE UNIVERSITY OF TEXAS AT AUSTIN

TABLE OF CONTENTS

LIST OF FIGURES

LIST OF TABLES

1 EXECUTIVE SUMMARY

The objective of this report is to set forth a group of time-domain models for the early-design stage study of shipboard power systems. These models are highly simplified abstractions of shipboard power system components. The motivation for the simplification is two-fold. First, at an early design stage it is doubtful if the parameters needed for a more detailed system representation would be available. A highly detailed simulation would be based on many assumptions leading to results which are no more indicative of actual performance than a highly simplified simulation. The second reason for the creation of highly simplified model is for the sake of computational speed, so that system simulations based on the component models will run at speeds compatible with the needs imposed by exploring the system behavior under a large variety of conditions.

The types of model simplifications used are three-fold. First, throughout this report average-value models are used. In particular, the switching of the power semiconductors is only represented on an average-value basis. Secondly, reduced-order models are typically used. Thus, high-frequency dynamics have been neglected. Simulation based on these models cannot be used to predict behaviors such as the initial response to a fault. In general, temporal predictions of features on a time scale of ~100 ms or less will not be reliable. The third simplification that has been made is that many components are represented in the abstract based on the operation goals of the component rather than on the details of what might physically be present.

The set of models provided herein is fairly extensive and adequate to serve as a basis for studying a variety of power system architectures. In particular, the set of models is currently being used to study a notional medium voltage ac shipboard power system, a notional high-frequency ac shipboard power system, and a notional dc shipboard power system. In order to support these studies, the models set forth include: turbines, turbine governors, wound-rotor synchronous machine based ac generators, generator paralleling controls, rectified wound-rotor synchronous machine based dc generation systems, ac input permanent magnet synchronous machine based propulsion drives, dc input permanent magnet synchronous machine based propulsion drives, hydrodynamic models, ac and dc pulsed load models, isolated dc/dc conversion models, dc loads, non-isolated dc/ac inverter modules, ac loads, active zonal rectifiers, circuit breakers and controls, as well as a variety of supporting components.

For the purposes of brevity and because of the resources available, model validation results are not presented herein. However, comments on model maturity have been included with each component to provide the reader with a sense of the degree of model confidence for each component.

Finally, the reader should be aware that a follow-on report will be delivered in the January 2014 time frame. This report will include an update of the models presented herein, but also include examples of their application in the simulation of notional medium voltage ac, high-frequency ac, and dc shipboard power distribution systems.

2 INTRODUCTION

As stated in the Executive Summary, this report is essentially a collection of simplified component models. The models are normally reduced-order in nature, and those models which correspond to components which include power electronics only represent the switching of the power semiconductor devices on an average value basis. The component models often are based on the intention of component rather than its physical implementation. Because of this, it is doubtful that temporal features on a time scale of 100 ms or less are accurately predicted.

The organization of this report is as follows. In Section 3 – Nomenclature, the format for the documentation of each model is explained. The next section, Nominal System Architectures, details three notional power systems in order to provide context and motivation for those models selected to be in this report. The bulk of the report is in Section 5 – Component Models. Therein, each component model is individually discussed.

3 MODEL REPORTING STRUCTURE

The model structure adopted in this work consists of describing the model in terms of its mathematical definition. To this end, the model reporting structure consists of a description of the model inputs, outputs, parameters, interface equations, and states before describing the mathematical model equations. The input and output definition refers to the model time domain structure and not the component functionality. The next aspect of the model reporting structure is to address the status of the validation of each model. The final area of the model reporting is the relevant references.

Inputs:
The inputs consist of the variables that are needed to either compute the time derivatives of the state variables of the model or to compute the output variables.

Outputs:
The model outputs are those variables associated with the model which are typically of direct interest to the system analyst or are typically needed by other system components. These variables are typically computed based on model state variables and/or model input variables.

Parameters:
The model parameters are those quantities in the model which are constant for a given component, such as control gains and circuit element values.

Interface Equations:
The interface equations are the algebraic equations that define the outputs of the component as a function of inputs and states that are solved by the system solver.

States:
The model states are those variables which are governed by ordinary differential equations and hence cannot change instantaneously. A major element of the every model is the computation of the time derivative of the state variables in terms of the inputs and states.

Model Equations:
The model equations are a listing of the mathematical equations within the model that are needed to obtain the time-derivatives of the state variables and output variables in terms of the input variables and state variables.

Validation:
The model validation section provides comments on the model maturity and the confidence level of the appropriate model.

References:
The reference section lists the applicable references for the presented component model.

4   NOMINAL SYSTEM ARCHITECTURES

The component models discussed herein were motivated by the desire to study a variety of shipboard power systems. All of these systems utilize the notional system architecture depicted in Fig. 5.1.1. There are two main and two auxiliary power generation modules (main PGM1, main PGM2, auxiliary PGM1, and auxiliary PGM2). These power generation modules feed starboard and port side busses that form a ring bus through the bow and stern cross-hull disconnects. The generation systems consist of wound rotor synchronous machines (WRSM) driven by gas turbines. This distribution bus feeds four types of loads. There is a starboard and a port side propulsion motor as well as a high power pulsed load. The propulsion motors include a variable speed drive (VSD) that represents the power converters between the motor and the bus. The last load type is a zonal load that represents the ship service electrical components throughout the ship. Each zonal load center is in itself a small network. These zonal load centers differ based on the architecture of the notional system.
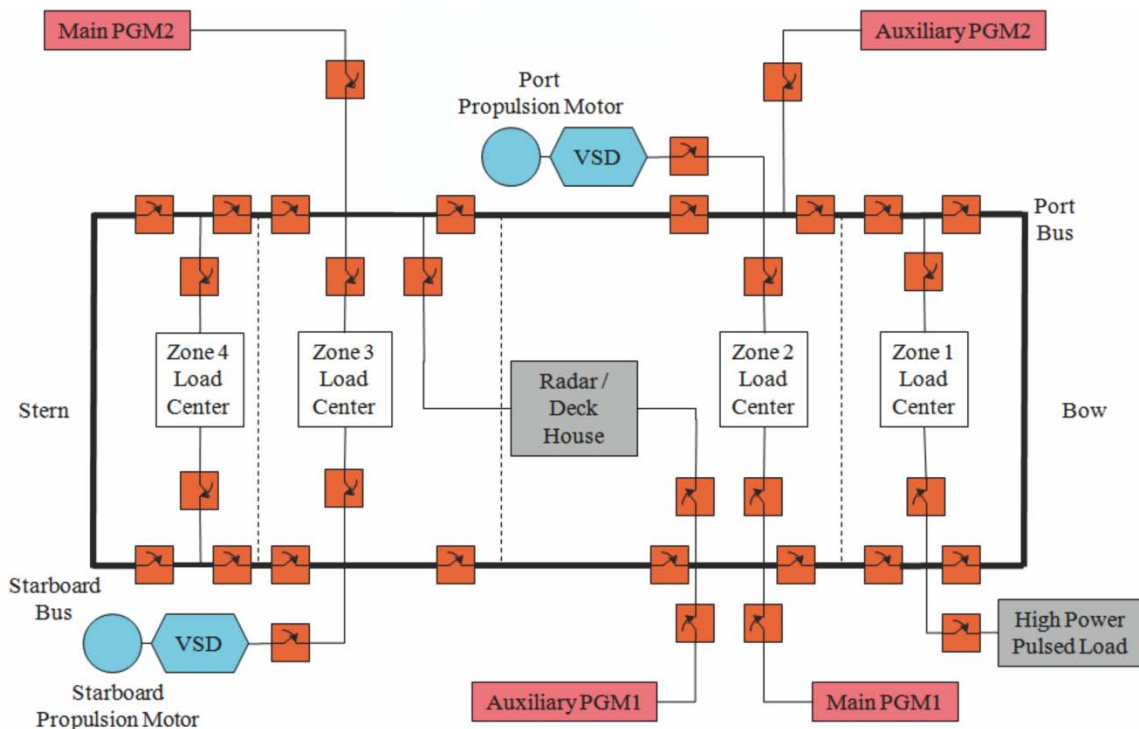
Fig. 4.1.1: Notional Power System.

There are three instantiations of this notional power system considered. The first is a Medium Voltage AC (MVAC) power system. This zonal load center for this system is depicted in Fig. 5.1.2 and consists of ac distribution busses on the starboard and port side. The ac loads can therefore be fed from the ac bus through a transformer (T) while the zonal dc loads are fed through a zonal active rectifier (ZAR).
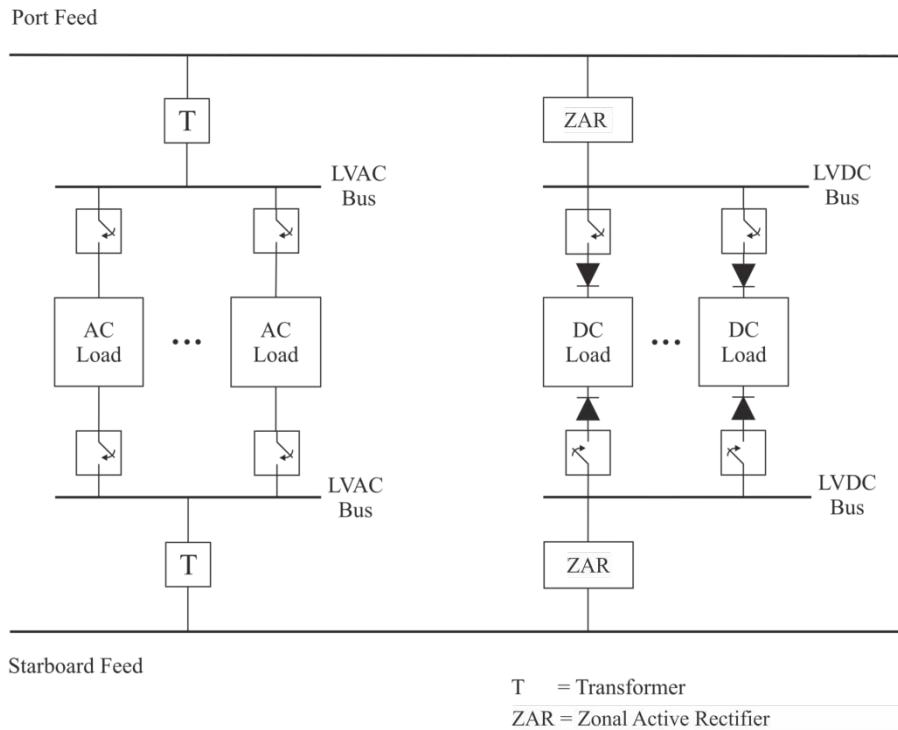
Fig. 4.1.2: Notional MVAC Zone.

The second version of the notional power system is a High Frequency AC (HFAC) power system. The zonal load center for this system is depicted in Fig. 5.1.3. Like the MVAC version, the HFAC version has ac distribution busses on the starboard and port side. The high frequency ac loads are fed from the ac bus through transformers (T) while the dc loads are fed through zonal active rectifier (ZAR) modules like in the MVAC system. Low frequency ac loads are fed off of the low voltage dc bus (LVDC) through non-isolated inverter modules (NIMs).
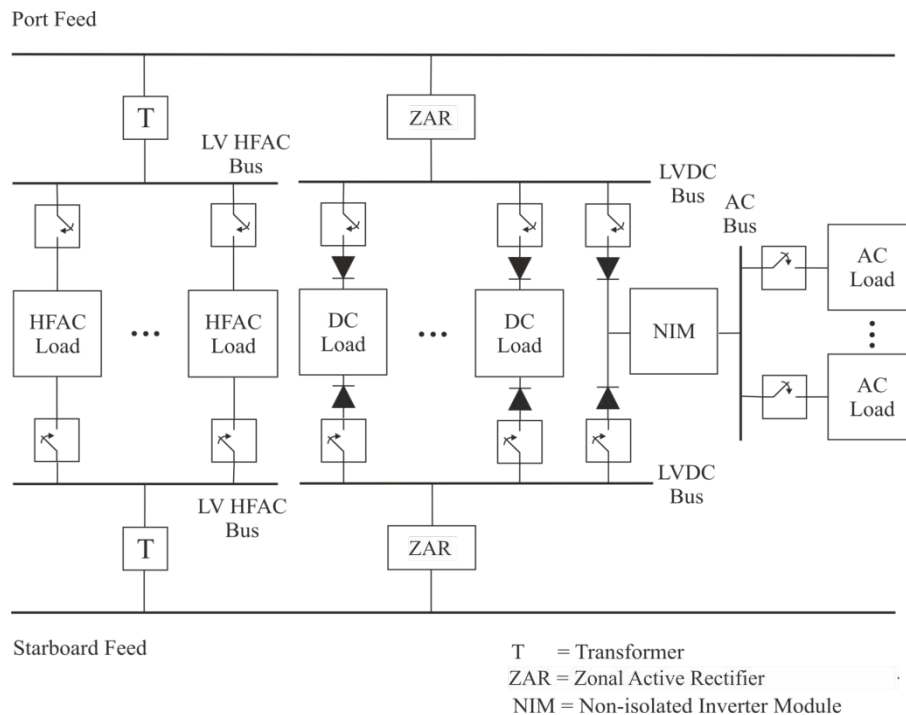
Fig. 4.1.3: Notional HFAC Zone.

8

The third instantiation of the notional power system is a Medium Voltage DC (MVDC) power system. The zonal load center for the MVDC system is depicted in Fig. 5.1.4. The starboard and port busses are dc busses that feed the dc loads through isolated dc/dc converters (IDCDC). Low-frequency (60 Hz) ac loads are fed through a non-isolated inverter module (NIM).

Fig. 4.1.4: Notional MVDC Zone.

5 COMPONENT MODELS

In this section, each of the component models needed to represent the MVAC, HFAC, and MVDC systems is represented.

5.1 Synchronous Reference Frame Estimator

The ac systems used herein feature multiple synchronous machines. Since the network equations must be solved in a single synchronous reference frame, the position of this reference frame must be defined. This model defines the position of the synchronous reference frame [5.1.1]. Note that this 'model' is different than most of the models in this report in that it does not represent a physical component. Rather, it defines the synchronous reference frame which is used for system analysis purposes. Nevertheless, it will be treated as if it were a component model for documentation purposes.

Inputs:
ω_{rAG} Vector of angular electrical speeds of all active generators (rad/s)

Outputs:
ω_e The estimated angular speed of the synchronous reference frame (rad/s)

Parameters:
P_{bAG} Vector of base power rating of all active generators (W)

Interface Equations:
None

States:
None

Model Equations:
The angular speed of the synchronous reference frame is a weighted average of the rotor speeds of all of the active generators. The weighting factor used is the base power of each generator. The calculation of the synchronous reference frame speed is found using

$$\omega_e = \frac{\sum_{i \in AG} P_{bAG,i} \omega_{rAG,i}}{\sum_{i \in AG} P_{bAG,i}} \tag{5.1.1}$$

Validation:
This is not a component, but rather a definition. Hence validation is not relevant.

References:
[5.1.1] P. Krause, O. Wasynczuk, S. Sudhoff, and S. Pekarek, "Analysis of Electric Machinery and Drive Systems," 3rd Edition, New York: John Wiley and Sons/IEEE Press, 2013.

5.2 AC WRSM Generator Model

The ac wound rotor synchronous machine model in this work is that of a wound-field synchronous machine with two q-axis damper windings and one d-axis damper winding. The model is defined in [5.2.1] and outlined herein. The reduced order of the model refers to the neglecting of the fast stator dynamics in the model definition. The structure of the model is as follows.

Inputs:

$\mathbf{v}_{qds}^e$ A vector of q- and d-axis terminal voltages (v_{qs}^e and v_{ds}^e) in the synchronous ref. frame (V)

ω_{rm} The mechanical rotor speed (rad/s)

v_{fd} The referred field voltage (V)

ω_e The radian frequency of the synchronous reference frame (rad/s)

Outputs:

$\mathbf{i}_{qds}^e$ A vector of q- and d-axis currents (i_{qs}^e and i_{ds}^e) into the machine in the synchronous ref. frame (A)

T_e The electrical torque of the machine (positive for motor operation) (Nm)

i_{fd} The referred field current into the machine (A)

Parameters:

r_s The referred resistance of the stator windings (Ω)

r_{kq1} The referred resistance of the 1st q-axis damper winding (Ω)

r_{kq2} The referred resistance of the 2nd q-axis damper winding (Ω)

r_{fd} The referred resistance of the d-axis field winding (Ω)

r_{kd} The referred resistance of the d-axis damper winding (Ω)

L_{mq} The q-axis mutual inductance (H)

L_{md} The d-axis mutual inductance (H)

L_{lkq1} The referred leakage inductance of the 1st q-axis damper winding (H)

L_{lkq2} The referred leakage inductance of the 2nd q-axis damper winding (H)

L_{lfd} The referred leakage inductance of the d-axis field winding (H)

L_{lkd} The referred leakage inductance of the d-axis damper winding (H)

Interface Equations:

The interface equation for the generator may be expressed

$$\mathbf{v}_{qds}^e = \underbrace{\begin{bmatrix} Z_{qq}^e & Z_{qd}^e \\ Z_{dq}^e & Z_{dd}^e \end{bmatrix}}_{\mathbf{Z}_{qd}^e} \mathbf{i}_{qds}^e + \underbrace{\begin{bmatrix} e_q^{"e} \\ e_d^{"e} \end{bmatrix}}_{\mathbf{e}_{qd}^{"e}} \tag{5.2.1}$$

where

$$Z_{qq}^e = r_s - \frac{\omega_r}{2}\sin(2\delta)\left(L_d'' - L_q''\right) \qquad (5.2.2)$$

$$Z_{qd}^e = \omega_r\left(L_d'' - \left(L_d'' - L_q''\right)\sin(\delta)^2\right) \qquad (5.2.3)$$

$$Z_{dq}^e = r_s + \frac{\omega_r}{2}\sin(2\delta)\left(L_d'' - L_q''\right) \qquad (5.2.4)$$

$$Z_{dd}^e = \omega_r\left(-L_q'' - \left(L_d'' - L_q''\right)\sin(\delta)^2\right) \qquad (5.2.5)$$

and

$$e_q''^e = \omega_r\left(\sin(\delta)\lambda_q'' + \cos(\delta)\lambda_d''\right) \qquad (5.2.6)$$

$$e_d''^e = \omega_r\left(-\cos(\delta)\lambda_q'' + \sin(\delta)\lambda_d''\right) \qquad (5.2.7)$$

In (5.2.2) through (5.2.7), δ is the torque angle which is a state. The impedances in (5.2.2) through (5.2.5) have units of Ohms and the voltages in (5.2.6) through (5.2.7) have units of V. In (5.2.2) through (5.2.7),

$$L_q'' = L_{ls} + \left(\frac{1}{L_{mq}} + \frac{1}{L_{lkq1}} + \frac{1}{L_{lkq2}}\right)^{-1} \qquad (5.2.8)$$

$$L_d'' = L_{ls} + \left(\frac{1}{L_{md}} + \frac{1}{L_{lkd}} + \frac{1}{L_{lfd}}\right)^{-1} \qquad (5.2.9)$$

and

$$\lambda_q'' = \frac{L_{mq}\left(\dfrac{\lambda_{kq1}}{L_{lkq1}} + \dfrac{\lambda_{kq2}}{L_{lkq2}}\right)}{1 + \dfrac{L_{mq}}{L_{lkq1}} + \dfrac{L_{mq}}{L_{lkq2}}} \qquad (5.2.10)$$

$$\lambda_d'' = \frac{L_{md}\left(\dfrac{\lambda_{kd}}{L_{lkd}} + \dfrac{\lambda_{fd}}{L_{lfd}}\right)}{1 + \dfrac{L_{md}}{L_{lkd}} + \dfrac{L_{md}}{L_{lfd}}} \qquad (5.2.11)$$

Model States:
δ Torque angle (rad)

λ_{kq1} The referred Flux linkage of 1st q-axis damper winding (Vs)

λ_{kq2} The referred Flux linkage of 2nd q-axis damper winding (Vs)

λ_{fd} The referred Flux linkage of d-axis field winding (Vs)

λ_{kd} The referred Flux linkage of d-axis damper winding (Vs)

Model Equations:

  The time derivative of the torque angle is calculated as

$$\frac{d\delta}{dt} = \omega_r - \omega_e \tag{5.2.12}$$

The time derivatives of the rotor states are found using the sequence

$$\mathbf{i}_{qds}^e = \mathbf{Z}_{qd}^{e\ -1}\left(\mathbf{v}_{qds}^e - \mathbf{e}_{qd}^{"e}\right) \tag{5.2.13}$$

$${}^e\mathbf{K}^r = \begin{bmatrix} \cos(\delta) & -\sin(\delta) \\ \sin(\delta) & \cos(\delta) \end{bmatrix} \tag{5.2.14}$$

$$\mathbf{i}_{qds}^r = {}^e\mathbf{K}^r\mathbf{i}_{qds}^e \tag{5.2.15}$$

$$i_{kq1} = \frac{\left(L_{lkq1}\lambda_{kq2} - L_{mq}\lambda_{kq1} + L_{mq}\lambda_{kq2} - L_{lkq1}L_{mq}i_{qs}^r\right)}{L_{lkq2}\left(L_{lkq1} + L_{mq}\right) + L_{lkq1}L_{mq}} \tag{5.2.16}$$

$$i_{kq2} = \frac{\left(L_{lkq2}\lambda_{kq1} - L_{mq}\lambda_{kq2} + L_{mq}\lambda_{kq1} - L_{lkq2}L_{mq}i_{qs}^r\right)}{L_{lkq1}\left(L_{lkq2} + L_{mq}\right) + L_{lkq2}L_{mq}} \tag{5.2.17}$$

$$i_{fd} = \frac{\left(L_{lfd}\lambda_{kd} - L_{md}\lambda_{fd} + L_{md}\lambda_{kd} - L_{lfd}L_{md}i_{ds}^r\right)}{L_{lkd}\left(L_{lfd} + L_{md}\right) + L_{lfd}L_{md}} \tag{5.2.18}$$

$$i_{kd} = \frac{\left(L_{lkd}\lambda_{fd} - L_{md}\lambda_{kd} + L_{md}\lambda_{fd} - L_{lkd}L_{md}i_{ds}^r\right)}{L_{lfd}\left(L_{lkd} + L_{md}\right) + L_{lkd}L_{md}} \tag{5.2.19}$$

whereupon the time derivatives of the rotor states are found using

$$\frac{d\lambda_{kq1}}{dt} = -r_{kq1}i_{kq1} \tag{5.2.20}$$

$$\frac{d\lambda_{kq2}}{dt} = -r_{kq2}i_{kq2} \tag{5.2.21}$$

$$\frac{d\lambda_{fd}}{dt} = v_{fd} - r_{fd}i_{fd} \tag{5.2.22}$$

$$\frac{d\lambda_{kd}}{dt} = -r_{kd}i_{kd} \tag{5.2.23}$$

The stator flux linkages are found

$$\lambda_{qs} = L_{ls}i_{qs}^r + L_{mq}\left(i_{qs}^r + i_{kq1} + i_{kq2}\right) \tag{5.2.24}$$

$$\lambda_{ds} = L_{ls}i_{ds}^r + L_{md}\left(i_{ds}^r + i_{fd} + i_{kd}\right) \tag{5.2.25}$$

and the torque is calculated using

$$T_e = \frac{3}{2}\frac{P}{2}\left(\lambda_{ds}i_{qs}^r - \lambda_{qs}i_{ds}^r\right) \tag{5.2.26}$$

Validation:
    This model has been widely used in the power engineering community for decades. Note that this model does not include saturation. Further, it is a reduced order model, so initial fault response will not be correctly predicted.

References:
[5.2.1] P. Krause, O. Wasynczuk, S. Sudhoff, and S. Pekarek, "Analysis of Electric Machinery and Drive Systems," 3rd Edition, New York: John Wiley and Sons/IEEE Press, 2013.

5.3 AC WRSM Exciter Model

    The WRSM exciter model represents a rotating, rectifier type exciter based upon IEEEAC8B [5.3.1], and is depicted in Fig. 5.3.1.
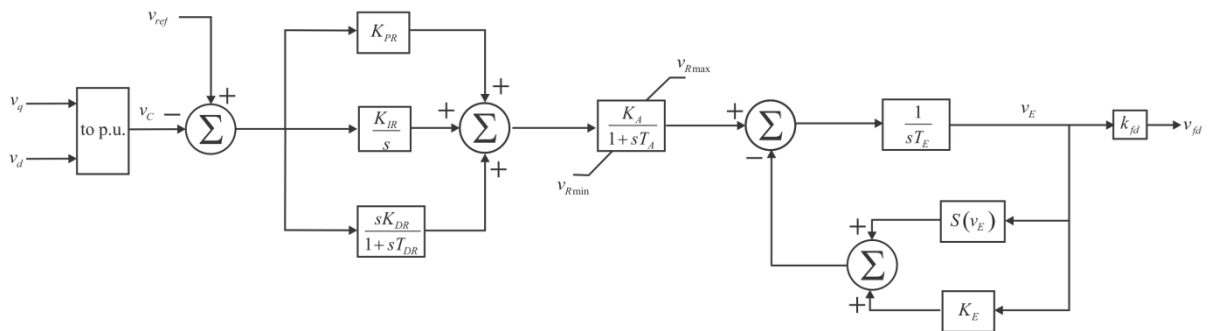
Fig. 5.3.1: Synchronous Generator Exciter Model.

The model structure is as follows.

Inputs:
v_q The q-axis terminal voltage (V)

v_d The *d*-axis terminal voltage (V)

Outputs:
v_{fd} The referred exciter voltage (V)

Parameters:
v_{ref} The per-unit line-line reference voltage (pu)

K_{PR} Automatic Voltage Regulator (AVR) proportional gain (pu)

K_{IR} AVR integral gain (pu)

K_{DR} AVR derivative gain (pu)

T_{DR} AVR derivative time constant (s)

K_A AVR power stage gain (pu)

T_A AVR power stage time constant (s)

$v_{R\max}$ AVR positive ceiling voltage (pu)

$v_{R\min}$ AVR negative ceiling voltage (pu)

T_E Exciter field time constant (s)

K_E Exciter field proportional gain (pu)

v_{rated} Rated line-line voltage of the synchronous machine (V)

Interface Equations:
None

Model Equations:
        The model equations are not explicitly given here as they are readily formulated from Fig. 5.3.1. The per-unit line-line measured voltage is obtained from the *q*- and *d*-axis voltages using

$$v_c = \sqrt{\frac{3}{2}} \frac{\sqrt{v_q^2 + v_d^2}}{v_{rated}} \qquad (5.3.1)$$

where v_{rated} is the rated rms line-neutral voltage of the synchronous machine.
        The saturation block in Fig. 5.3.1 is defined as

$$S(v_E) = Ae^{Bv_E} \qquad (5.3.2)$$

where A (1.0119) and B (0.875) are calculated using selected points on the voltage saturation curve, i.e. the open-circuit voltage vs. exciter field voltage curve.
        The physical field voltage is obtained by scaling V_E, the per-unit value of the field voltage.

$$v_{fd} = k_{fd}V_E \qquad (5.3.3)$$

where

$$k_{fd} = \frac{\sqrt{\frac{2}{3}} v_{rated} r_{fd}}{\omega_r L_{md}}$$

(5.3.4)

Validation:

This is a behavioral model commonly used in the power engineering community. However, it does not represent any physical excitation system.

References:

[5.3.1] L.M. Hajagos and M.J. Basler, "Changes to IEEE 421.5 recommended practice for excitation system models for power stability studies", IEEE/PES 2005 Meeting, San Francisco, CA.

5.4 AC Generator Real Time Synchronization Controller

The AC generator synchronization controller is used for MVAC and HFAC systems, where synchronization of paralleled generators is important. In MVAC and HFAC power distribution systems for an Electric Ship, multiple AC generators are present. Depending on the system operating mode, the overall system may break up into unconnected subsystems – for example unconnected starboard and port busses fed by separate AC generators. At some point, system reconfiguration may cause previously disconnected parts of the electrical distribution system to be interconnected. This may lead to large transients if the overall system is not properly synchronized. This section describes a supervisory controller called Real-Time Synchronization Controller (RTSC), which solves this problem by keeping all parts of the electrical distribution system synchronized at all times, even when they are not electrically connected. This requires both frequency and phase synchronization for all AC generators. The RTSC accomplishes this by augmenting the conventional frequency droop control for generators. At any given time, one interconnected subsystem is considered the reference subsystem and all other systems are target subsystems. The RTSC forces the target subsystems to be phase-synchronized with the reference subsystem. For more information on the RTSC see [5.4.1]. The discussion refers to a set of generators, each consisting of a gas turbine, as described in Section 5.5, connected to an AC WRSM generator, as described in Sections 5.1 through 5.3.

Inputs:

$\omega_{rm,ref}$ Reference turbine speed (pu)

P_i Output power of *i*th generator (W)

$\mathbf{v}_{qd,\text{ref}}$ A vector of *q*- and *d*-axis terminal voltages for the reference subsystem (V)

$\mathbf{v}_{qd,\text{target}}$ A vector of *q*- and *d*-axis terminal voltages for the target subsystem (V)

Outputs:

$\Delta\omega_{speed_i}$ Offset added to the common speed reference $\omega_{rm,ref}$ for the *i*th generator by the RTSC controller (pu)

Parameters:

D_i Droop setting of speed regulator for ith generator (pu)

P_{rated_i} Rated power of ith generator (W)

ω_I Cutoff frequency of Low-Pass Filter I (rad/s)

ω_{II} Cutoff frequency of Low-Pass Filter II (rad/s)

Model Equations:

In order for interconnected generators to operate reliably in parallel and share generated power in proportion to their respective power rating, speed regulators of generators are set in droop mode, so that the generator frequency has a constant proportional relationship to the turbine's output mechanical power, as shown in Fig. 5.4.1. This is accomplished by using appropriate settings for the speed governor equation. For explanation purposes it is assumed that the relationship between output power and speed offset may be adequately approximated as

$$G(s) = \frac{W(Xs+1)}{Ys+Z} \qquad (5.4.1)$$

A droop characteristic is obtained for $X = 0$, $Z = 1$ $W = K_D$ and the droop is given by

$$droop = \frac{1}{K_D} \qquad (5.4.2)$$

Using conventional droop control, an error proportional to the power delivered by the generators will be present in the generator speed and consequently in the electrical frequency. The RTSC frequency control introduces an offset in the droop function, so that in steady state the per-unit frequency is exactly one, as shown in Fig. 5.4.2. The offset in the droop function is created by adding a variable offset dynamically to the speed regulator reference in each generator. For the ith generator, the speed reference $\omega_{rm,ref}$ used is the single-shaft and twin-shaft gas turbine model (Fig. 5.5.1 and Fig. 5.5.2) is modified according to

$$\omega_{rm,ref_i}(t) = \omega_{rm,ref} + \Delta\omega_{speed_i}(t) \qquad (5.4.3)$$

where the frequency offset $\Delta\omega_{speed_i}(t)$ is the output of the RTSC controller for the ith generator. This quantity is given by
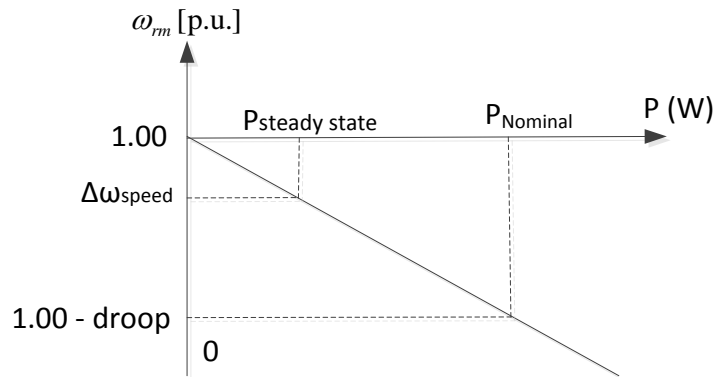
Fig. 5.4.1: Droop Function of Speed Regulator without RTSC.
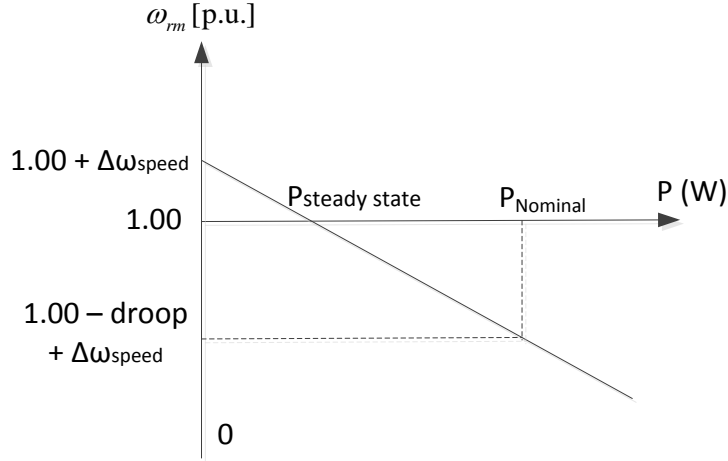
Fig. 5.4.2: Droop Function of Speed Regulator With RTSC.

$$\Delta\omega_{speed_i}(t) = D_i \cdot \frac{\displaystyle\sum_{j=1}^{n} K_{ij} P_j(t)}{\displaystyle\sum_{j=1}^{n} K_{ij} P_{rated\_j}} \qquad (5.4.4)$$

where D_i is the droop setting of the speed regulator in the ith Generator, P_{rated_j} is the rated active power of the jth Generator, $P_j(t)$ is the instantaneous output power of the jth Turbine Engine, K_{ij} represents the relationship between the Generators i and j: $K_{ij} = 1$ if the two generators are located in the same subsystem; $K_{ij} = 0$ if the two generators are located in different subsystems; n is the total number of generators in the ESPS. The RTSC controller can determine the values of K_{ij} based on the status of the circuit breakers on the power distribution busses. The ratio on the right hand side of (5.4.4) represents the percentage loading of the generators in the subsystem containing Generator i with respect to their combined rated power. When implementing the RTSC in an ESPS, one subsystem is chosen as the reference subsystem and the other subsystems are set as the target subsystems. The criterion to choose reference subsystem is that it should have the largest power rating among all subsystems. As the control is implemented in software, the reference subsystem can be chosen dynamically according to system operating state. The complete structure of the RTSC is shown in Fig. 5.4.3.
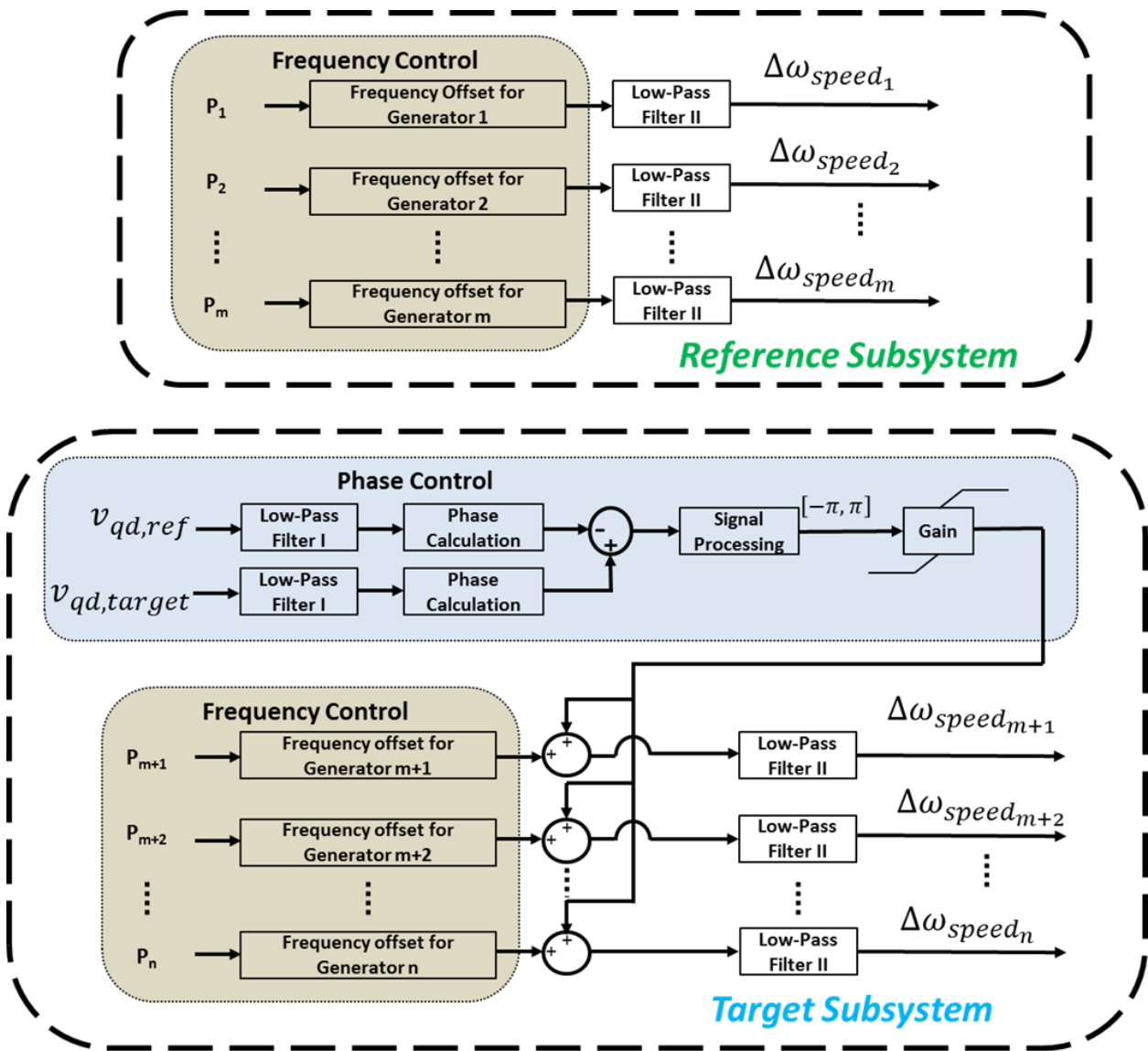
Fig. 5.4.3: Structure of the RTSC Consisting of Frequency Control and Phase Control.

In the figure only two subsystems are shown for simplicity: a reference subsystem, consisting of Generators $1 - m$, and a target subsystem, consisting of Generators $m+1 - n$. Additional subsystems would be shown as separate target subsystems. Both the reference and the target subsystem have Frequency Control, but only the target subsystem has Phase Control. The goal of Phase Control is to keep voltages of the target subsystem and the reference subsystem in phase at all times.

Inside the Frequency Control part of the controller, the frequency offset block calculates for each generator the frequency offset as a function of real power generated using (5.4.4). The frequency offset goes through a first-order lowpass filter called Low-Pass Filter II, having the form

$$G_{LPF-II}(s) = \frac{1}{1 + \dfrac{s}{\omega_{II}}} \tag{5.4.5}$$

19

For generators 1 – *m* belonging to the reference subsystem, this offset is added to the speed reference as in (5.4.3). For generators *m*+1 – *n* belonging to the target subsystem, the RTSC control includes also phase control.

In the Phase Control part of the controller, quantities $\mathbf{v}_{qd,\mathrm{ref}}$ and $\mathbf{v}_{qd,\mathrm{target}}$ are the vectors of *q*- and *d*-axis voltages for the reference and the target subsystem, respectively. Low-Pass Filter I (LPF-I) is a first-order lowpass filter used to eliminate the harmonics resulting from non-linear load current and it has the form

$$G_{LPF-I}(s) = \frac{1}{1+\dfrac{s}{\omega_I}} \tag{5.4.6}$$

For a generator having *q*-axis terminal voltage v_q and d-axis terminal voltage v_d, the Phase Calculation block calculates the absolute phase as

$$\theta_v = \operatorname{atan}2\left(v_d, v_q\right) \tag{5.4.7}$$

The phase difference between the target subsystem and the reference subsystem voltages is calculated as

$$\Delta\theta_v = \theta_{v,\mathrm{target}} - \theta_{v,\mathrm{ref}} \tag{5.4.8}$$

and sent to the Signal Processing block, which constrains its value from [-2π, 2π] to [-π, π] using phase wrap. The phase control offset is produced by the Gain block in Fig. 5.4.3 and is added to the frequency control offset. For details on the design of Low-Pass Filter I and Low-Pass Filter II, please refer to [5.4.1].

As a result of the RTSC control of Fig. 5.4.3 in steady state all subsystems operate at the nominal frequency (p.u. frequency of one) and the voltages of all target subsystems are in phase with the reference subsystem.

Validation:

This component model is of a control, not of a physical component. Therefore, it has to be considered in terms of effectiveness, not fidelity. The reader is referred to [5.4.1] for a discussion of the effectiveness of this control.

References:
[5.4.1] E. Santi, and Y. Zhang, "Design of Real-Time Synchronization Controller in Electric Ship Power Systems," ESRDC Report, 2013.
[5.4.2] W.I. Rowen, "Simplified Mathematical Representations of Heavy-duty Gas Turbines", Journal of Engineering for Power, Vol. 105, 1983.

5.5 Generic Prime Mover Model

The gas turbine models used in this work consist of speed and acceleration control loops. The temperature control often associated with this type of gas turbine representation is omitted herein based upon the assumption that the critical turbine temperature will not be reached since

temperature changes occur mostly during the startup of the turbine. The transfer function representing the speed governor allows for either droop or isochronous control. Setting the speed governor transfer function coefficient X=0 results in droop control where the output of the governor is directly proportional to the speed error, as can be seen in the turbine model diagrams in Fig. 5.5.1 and Fig. 5.5.2.

5.5.1 Single-shaft Gas Turbine

The single-shaft gas turbine model is depicted in Fig. 5.5.1.

The structure of the turbine model is as follows.

Inputs:
$\omega_{rm,ref}$ Reference speed (pu)
ω_{rm} Turbine speed (pu)

Outputs:
T_m Output torque (Nm)

Parameters:
W,X,Y,Z   Speed governor parameters (pu)

$F_{l,\max}$ Maximum fuel limit (pu)
$F_{l,\min}$ Minimum fuel limit (pu)
K_{ia} Acceleration parameter (pu)
K_a Acceleration parameter (pu)
K_{fla} Fuel control parameter (pu)
K_{flb} Fuel control parameter (pu)
a,b,c   Valve control parameters (pu)
τ_{fs} Fuel system time constant (s)
T_c Combustor time delay (s)
τ_{cp} Compressor time constant (s)

Interface Equations:
None
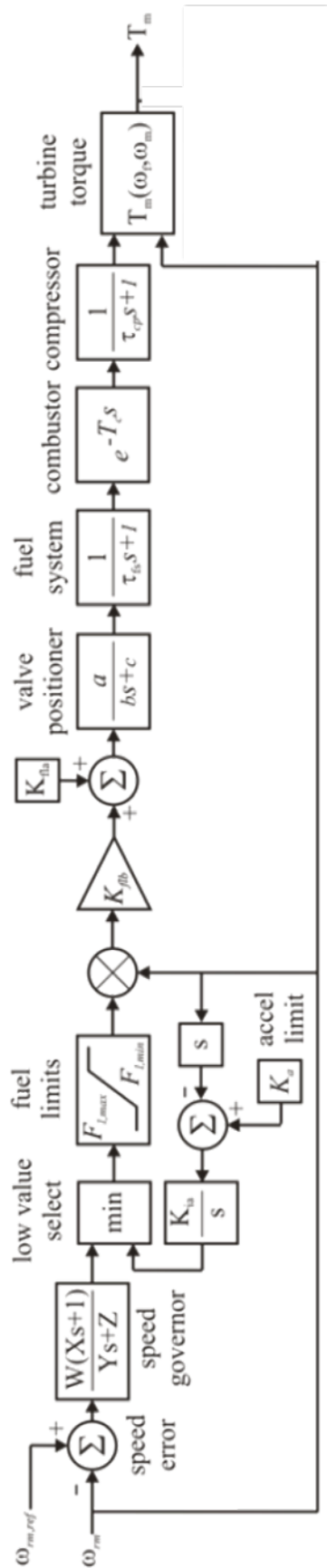
Fig. 5.5.1: Generic Single-Shaft Gas Turbine Model [5.5.1].

Model Equations:

The per unit turbine speed is found by dividing by the nominal speed of the turbine. The output torque, T_m in per-unit, is calculated using the turbine torque function [5.5.1]

$$T_{m,pu} = \frac{1}{K_{flb}}\left(\omega_f - K_{fla}\right) + \frac{1}{2}\left(1 - \omega_{rm}\right) \qquad (5.5.1)$$

where ω_f is the output of the compressor block and the turbine shaft speed, ω_{rm}, is in per-unit. The actual torque in Nm is obtained using

$$T_{m,\text{Nm}} = k_t T_{m,pu} \qquad (5.5.2)$$

where

$$k_t = \frac{P_{\text{nominal}}}{\omega_{\text{nominal}}} \qquad (5.5.3)$$

This gas turbine model and the overall parameters of the model can be different for gas turbines built by different manufacturers; however, the general model structure is an adequate representation for describing the dynamic behavior of a single-shaft gas turbine.

Validation:

The validity of this model is discussed in [5.5.1].

References:
[5.5.1] W.I. Rowen, "Simplified mathematical representations of heavy-duty gas turbines", Journal of Engineering for Power, Vol. 105, 1983.

5.5.2 Twin-shaft Gas Turbine

The model for the twin-shaft gas turbine is similar to the single-shaft gas turbine but with an additional control loop for the engine speed [5.5.2] and is depicted in Fig. 5.5.2.

Inputs:

$\omega_{rm,ref}$ Reference turbine speed (pu)

ω_{rm} Turbine speed (pu)

$\omega_{g,ref}$ Reference engine speed (pu)

ω_g Engine speed (pu)

Outputs:

T_m Output torque (Nm)
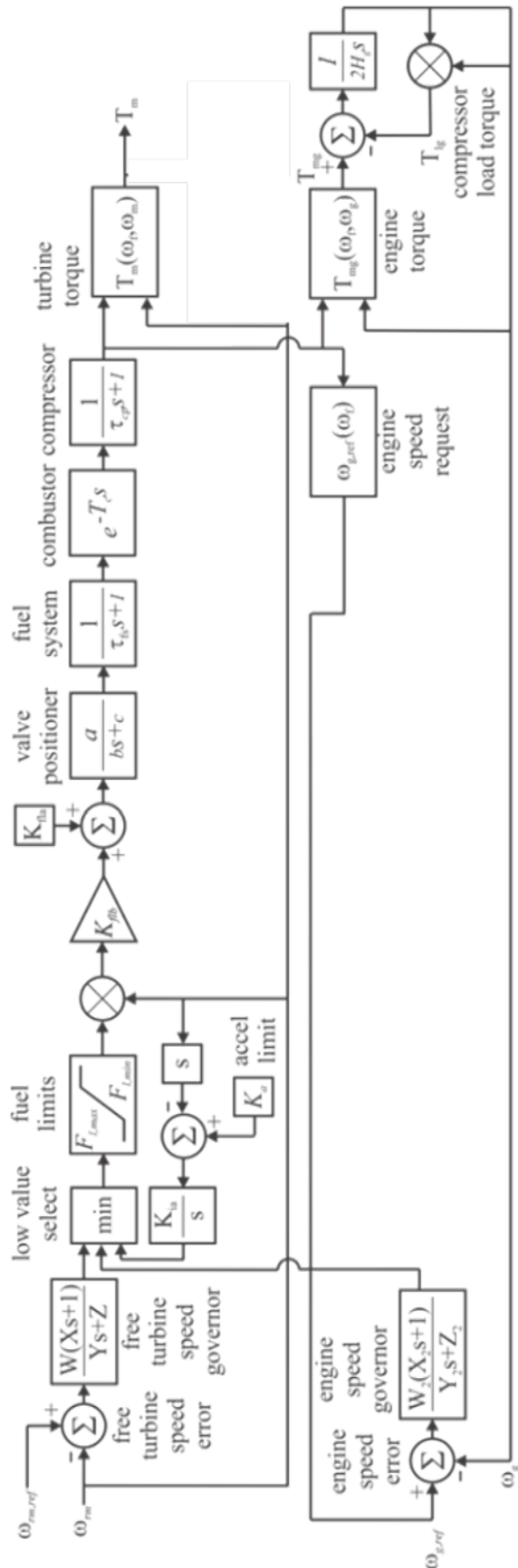
Fig. 5.5.2: Generic Twin-Shaft Gas Turbine Model.

Parameters:

W,X,Y,Z — Turbine speed governor parameters (pu)

W_2, X_2, Y_2, Z_2 — Engine speed governor parameters (pu)

$F_{l,\max}$ — Maximum fuel limit (pu)

$F_{l,\min}$ — Minimum fuel limit (pu)

K_{ia}, K_a — Acceleration parameters (pu)

K_{fla}, K_{flb} — Fuel control parameters (pu)

a,b,c — Valve control parameters (pu)

τ_{fs} — Fuel system time constant (s)

T_c — Combustor time delay (s)

τ_{cp} — Compressor time constant (s)

H_g — Engine shaft inertial constant (pu)

Interface Equations:
None

Model Equations:

The per-unit turbine speeds are converted to per-unit by dividing by the nominal turbine speed. The per-unit torque is converted to Nm using (5.5.2) and (5.5.3).

The free turbine torque is calculated

$$T_m = \frac{1}{K_{flb}}\left(\omega_f - K_{fla}\right) + 0.6\left(1 - \omega_{rm}\right) \tag{5.5.4}$$

The engine torque is calculated

$$T_{mg} = \frac{1}{K_{flb}}\left(\omega_f - K_{fla}\right) + 3\left(1 - \omega_g\right) \tag{5.5.5}$$

The engine speed request is calculated

$$\omega_{g,ref} = p_1\omega_f + p_2 \tag{5.5.6}$$

Validation:

The validity of this model is discussed in [5.5.2].

References:

[5.5.2] L.N. Hannet, G. Jee, and B. Fardanesh, "A governor/turbine model for a twin-shaft combustion turbine," IEEE Transactions on Power Systems, Vol. 10, no.1, pp. 133-140.

5.6   DC WRSM Generator Model

The dc WRSM model is depicted in Fig. 5.6.1 and consists of a WRSM connected to load commutated rectifier through an ac circuit breaker (CB). The component model is set forth in [5.6.1] and outlined herein.
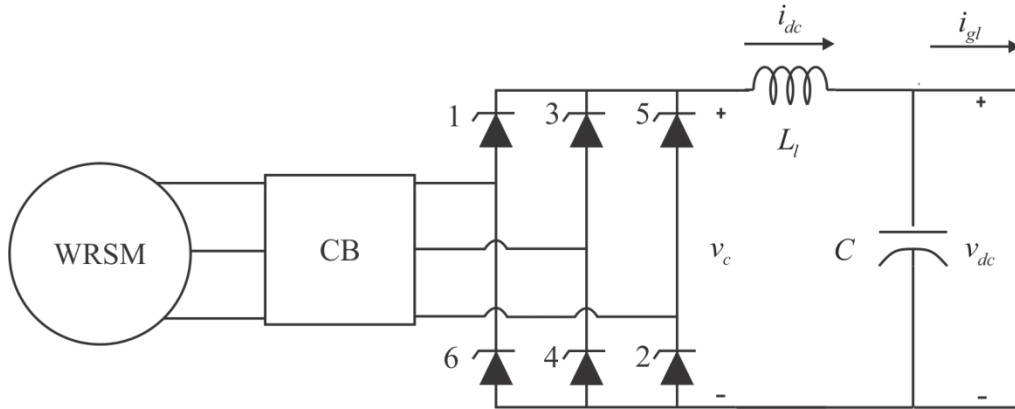
Fig. 5.6.1: Synchronous Machine Fed Load Commutated Converter.

The structure of the model is as follows:

Inputs:

i_{gl} The dc load current out of the generator (A)

ω_{rm} The mechanical rotor speed of the machine (rad/s)

v_{fd} The referred field voltage (V)

o_{gcb}^{*} The desired status of the generator circuit breaker

Outputs:

v_{dc} The dc output voltage of the generator (V)

T_e The electrical torque of the machine (positive for motor operation) (Nm)

i_{fd} The referred field current into the machine (A)

Parameters:

$v_{dc,\min}$ The dc bus voltage threshold (V)

i_{glf} The load current fault threshold (A)

L_l DC link inductance (H)

C DC link capacitance (F)

r_s The resistance of the stator windings (Ω)

r_{kq1} The referred resistance of the 1st q-axis damper winding (Ω)

r_{kq2} The referred resistance of the 2nd q-axis damper winding (Ω)

r_{fd} The referred resistance of the d-axis field winding (Ω)

r_{kd} The referred resistance of the d-axis damper winding (Ω)

L_{mq} The q-axis mutual inductance (H)

L_{md} The *d*-axis mutual inductance (H)

L_{lkq1} The referred leakage inductance of the 1st *q*-axis damper winding (H)

L_{lkq2} The referred leakage inductance of the 2nd *q*-axis damper winding (H)

L_{lfd} The referred leakage inductance of the *d*-axis field winding (H)

L_{lkd} The referred leakage inductance of the *d*-axis damper winding (H)

Interface Equations:
None

Model States:

v_{dc} The dc output voltage of the generator (V)

i_{dc} The dc current through the dc link inductor (V)

λ_{kq1} The referred Flux linkage of 1st *q*-axis damper winding (Vs)

λ_{kq2} The referred Flux linkage of 2nd *q*-axis damper winding (Vs)

λ_{fd} The referred Flux linkage of *d*-axis field winding (Vs)

λ_{kd} The referred Flux linkage of *d*-axis damper winding (Vs)

Model Equations:

The model equations for this component are broken in to six subsections. First, the subtransient model is defined, followed by the calculation of the firing and commutation angles. The third section considers the calculation of the stator currents and the fourth and fifth sections define the machine and dc link dynamics respectively. The final subsection relates to the exciter model.

5.6.1 Subtransient Model

It is useful to represent the reduced-order synchronous machine stator voltage equations in voltage-behind-reactance form utilizing subtransient quantities when coupled with a rectifier. For a synchronous machine with two *q*-axis damper windings and one *d*-axis damper winding, the subtransient inductances and flux linkages are expressed [5.6.1]

$$L_q^{"} = L_{ls} + \left(\frac{1}{L_{mq}} + \frac{1}{L_{lkq1}} + \frac{1}{L_{lkq2}} \right)^{-1} \tag{5.6.1}$$

$$L_d^{"} = L_{ls} + \left(\frac{1}{L_{md}} + \frac{1}{L_{lkd}} + \frac{1}{L_{lfd}} \right)^{-1} \tag{5.6.2}$$

$$\lambda_q^{"} = \frac{L_{mq} \left(\dfrac{\lambda_{kq1}}{L_{lkq1}} + \dfrac{\lambda_{kq2}}{L_{lkq2}} \right)}{1 + \dfrac{L_{mq}}{L_{lkq1}} + \dfrac{L_{mq}}{L_{lkq2}}} \tag{5.6.3}$$

27

$$\lambda_d'' = \frac{L_{md}\left(\dfrac{\lambda_{kd}}{L_{lkd}} + \dfrac{\lambda_{fd}}{L_{lfd}}\right)}{1 + \dfrac{L_{md}}{L_{lkd}} + \dfrac{L_{md}}{L_{lfd}}} \tag{5.6.4}$$

5.6.2 Firing Angle and Commutation Angle Calculations

The second step in modeling this system is the calculation of the firing angle and commutation angle. Assuming that that the circuit breaker is closed, the calculation of the firing angle (β) relative to rotor position is discussed in [5.6.1] and outlined herein. For uncontrolled operation the firing angle relative to rotor position is equal to β_{min} which is found by solving

$$\sqrt{3}\left(\lambda_q'' \cos\beta_{min} + \lambda_d'' \sin\beta_{min}\right) + 2\hat{i}_{dc}\left(L_q'' - L_d''\right)\sin\left(2\beta_{min} - \frac{\pi}{3}\right) = 0 \tag{5.6.5}$$

An intermediate variable K is the found by solving

$$K = \sqrt{3}\left(-\lambda_q'' \sin\beta + \lambda_d'' \cos\beta\right) + \left[\left(L_d'' - L_q''\right)\cos\left(2\beta + \frac{2\pi}{3}\right) - \frac{1}{2}\left(L_q'' + L_d''\right)\right]\hat{i}_{dc} \tag{5.6.6}$$

Whereupon the commutation angle, μ, is found by solving

$$K - \sqrt{3}\left[-\lambda_q'' \sin\left(\beta + \mu\right) + \lambda_d'' \cos\left(\beta + \mu\right)\right] -$$
$$\left[\left(L_q'' - L_d''\right)\cos\left(2\beta + 2\mu - \frac{2\pi}{3}\right) + \frac{1}{2}\left(L_q'' + L_d''\right)\right]\hat{i}_{dc} = 0 \tag{5.6.7}$$

In the event that the circuit breaker is open, then β_{min}, K, and μ can all be set to zero as they are unused.

5.6.3 Calculation of Stator Currents

The next step in the modeling of the system is the calculation of the average q and d axis currents. In the case that the circuit breaker is open, the q- and d-axis currents are set to zero. If the circuit breaker is closed, they are calculated using the following procedure.

The average values of the q and d axis currents are broken into commutation and conduction components. First, the conduction components are obtained using

$$\hat{i}_{qs,cond} = \frac{2\sqrt{3}}{\pi}\hat{i}_{dc}\left[\cos\left(\beta + \frac{2\pi}{3}\right) - \cos\left(\beta + \mu + \frac{\pi}{3}\right)\right] \tag{5.6.8}$$

$$\hat{i}_{ds,cond} = \frac{2\sqrt{3}}{\pi}\hat{i}_{dc}\left[\sin\left(\beta + \frac{2\pi}{3}\right) - \sin\left(\beta + \mu + \frac{\pi}{3}\right)\right] \tag{5.6.9}$$

28

During the interval following the firing of valve 3, the *a*-phase current is given by

$$
\begin{aligned}
i_{as}\left(\tilde{\theta}_r\right) = & \frac{K+\sqrt{3}\left(\lambda_q^{"}\sin\left(\tilde{\theta}_r+\beta\right)-\lambda_d^{"}\cos\left(\tilde{\theta}_r+\beta\right)\right)}{\left(L_q^{"}+E_d^{"}\right)-\left(L_q^{"}-L_d^{"}\right)\cos\left(2\tilde{\theta}_r+2\beta\right)} \\
& -\frac{\left[\left(L_q^{"}-L_d^{"}\right)\cos\left(2\tilde{\theta}_r+2\beta-\dfrac{2\pi}{3}\right)+\dfrac{1}{2}\left(L_q^{"}+L_d^{"}\right)\right]\hat{i}_{dc}}{\left(L_q^{"}+L_d^{"}\right)-\left(L_q^{"}-L_d^{"}\right)\cos\left(2\tilde{\theta}_r+2\beta\right)}
\end{aligned}
\tag{5.6.10}
$$

where $\tilde{\theta}_r$ is the electrical rotor position offset such that valve 3 fires when $\tilde{\theta}_r = 0$. The *q* and *d* axis currents can be expressed in terms of the *a*-phase current as

$$
i_{qs}\left(\tilde{\theta}_r\right)=\frac{2\sqrt{3}}{3}\left[-i_{as}\left(\tilde{\theta}_r\right)\sin\left(\tilde{\theta}_r+\beta\right)-\hat{i}_{dc}\sin\left(\tilde{\theta}_r+\beta+\frac{\pi}{3}\right)\right]
\tag{5.6.11}
$$

$$
i_{ds}\left(\tilde{\theta}_r\right)=\frac{2\sqrt{3}}{3}\left[i_{as}\left(\tilde{\theta}_r\right)\cos\left(\tilde{\theta}_r+\beta\right)+\hat{i}_{dc}\cos\left(\tilde{\theta}_r+\beta+\frac{\pi}{3}\right)\right]
\tag{5.6.12}
$$

Therefore, the commutation component of the average *q* and *d* axis currents is given by

$$
\hat{i}_{qs,com}=\frac{\mu}{4\pi}\left[i_{qs}\left(0\right)+4i_{qs}\left(\frac{\mu}{4}\right)+2i_{qs}\left(\frac{\mu}{2}\right)+4i_{qs}\left(\frac{3\mu}{4}\right)+i_{qs}\left(\mu\right)\right]
\tag{5.6.13}
$$

$$
\hat{i}_{ds,com}=\frac{\mu}{4\pi}\left[i_{ds}\left(0\right)+4i_{ds}\left(\frac{\mu}{4}\right)+2i_{ds}\left(\frac{\mu}{2}\right)+4i_{ds}\left(\frac{3\mu}{4}\right)+i_{ds}\left(\mu\right)\right]
\tag{5.6.14}
$$

and the average *q* and *d* axis currents are found using

$$
\hat{i}_{qs}=\hat{i}_{qs,cond}+\hat{i}_{qs,com}
\tag{5.6.15}
$$

$$
\hat{i}_{ds}=\hat{i}_{ds,cond}+\hat{i}_{ds,com}
\tag{5.6.16}
$$

5.6.4 Machine Dynamics

The next step is to calculate the flux linkages, the derivative of flux linkages, and the electrical torque of the machine which can be written as

$$
\lambda_{qs}=L_q^{"}\hat{i}_{qs}+\lambda_q^{"}
\tag{5.6.17}
$$

$$
\lambda_{ds}=L_d^{"}\hat{i}_{ds}+\lambda_d^{"}
\tag{5.6.18}
$$

29

$$\frac{d\lambda_{kq1}}{dt} = \frac{-r_{kq1}}{L_{lkq1}}\left(\lambda_{kq1} - L_q''\hat{i}_{qs} - \lambda_q'' + L_{ls}\hat{i}_{qs}\right) \tag{5.6.19}$$

$$\frac{d\lambda_{kq2}}{dt} = \frac{-r_{kq2}}{L_{lkq2}}\left(\lambda_{kq2} - L_q''\hat{i}_{qs} - \lambda_q'' + L_{ls}\hat{i}_{qs}\right) \tag{5.6.20}$$

$$\frac{d\lambda_{kd}}{dt} = \frac{-r_{kd}}{L_{lkd}}\left(\lambda_{kd} - L_d''\hat{i}_{ds} - \lambda_d'' + L_{ls}\hat{i}_{ds}\right) \tag{5.6.21}$$

$$\frac{d\lambda_{fd}}{dt} = v_{fd} - \frac{r_{fd}}{L_{lfd}}\left(\lambda_{fd} - L_d''\hat{i}_{ds} - \lambda_d'' + L_{ls}\hat{i}_{ds}\right) \tag{5.6.22}$$

The electrical torque of the synchronous machine (positive for generator operation) is found using

$$T_e = -\frac{3}{2}\frac{P}{2}\left(\lambda_{ds}\hat{i}_{qs} - \lambda_{qs}\hat{i}_{ds}\right) \tag{5.6.23}$$

The mechanical dynamics of the synchronous machine generator are expressed

$$J_g\frac{d\omega_{rm}}{dt} = T_{pm} - T_e \tag{5.6.24}$$

where T_{pm} is the prime mover torque.

5.6.5 DC Link Dynamics

The dc link dynamics are computed by first computing the commutating inductance L_c is given by

$$L_c(\beta) = \frac{1}{2}\left(L_q'' + L_d''\right) + \left(L_d'' - L_q''\right)\sin\left(2\beta + \frac{\pi}{6}\right) \tag{5.6.25}$$

and the transient commutating inductance expressed

$$L_t(\beta) = L_q'' + L_d'' + \left(L_d'' - L_q''\right)\sin\left(2\beta - \frac{\pi}{6}\right) \tag{5.6.26}$$

The magnitude of the subtransient voltage is given by

$$E = |\omega_r|\sqrt{\left(\lambda_q''\right)^2 + \left(\lambda_d''\right)^2} \tag{5.6.27}$$

which is obtained from

$$e_q'' = \omega_r\lambda_d'' \tag{5.6.28}$$

$$e_d^{"} = -\omega_r \lambda_q^{"} \tag{5.6.29}$$

Next, the phase angle of the subtransient voltage is calculated as

$$\phi = \text{angle}\left(\lambda_d^{"} - j\lambda_q^{"}\right) \tag{5.6.30}$$

which is obtained from (5.6.28), (5.6.29), and

$$\phi = \text{angle}\left(e_q^{"} + je_d^{"}\right) \tag{5.6.31}$$

whereupon the firing angle relative to the voltage is given by

$$\alpha = \beta - \phi \tag{5.6.32}$$

The time derivative of the average dc current is expressed as

$$\frac{d\hat{i}_{dc}}{dt} = \begin{cases} \dfrac{\dfrac{3\sqrt{3}}{\pi}E\cos\alpha - \hat{v}_{dc} - \left(r_l + \dfrac{3}{\pi}\omega_r L_c\left(\beta\right)\right)\hat{i}_{dc}}{L_l + L_t\left(\beta\right)} & c_g \cdot \left((\hat{i}_{dc} > 0) + \left(\dfrac{3\sqrt{3}}{\pi}E\cos\alpha > \hat{v}_{dc}\right)\right) \\[2em] -k\hat{i}_{dc} & \overline{c_g \cdot \left((\hat{i}_{dc} > 0) + \left(\dfrac{3\sqrt{3}}{\pi}E\cos\alpha > \hat{v}_{dc}\right)\right)} \\[2em] \dfrac{-\hat{v}_{dc} - r_l\hat{i}_{dc}}{L_l} & \overline{c}_g \cdot (\hat{i}_{dc} > 0) \\[1em] -k\hat{i}_{dc} & \overline{c}_g \cdot (\hat{i}_{dc} \leq 0) \end{cases} \tag{5.6.33}$$

In (5.6.33), k is an artificial constant used to drive the dc link current to zero.
The time derivative of the capacitor voltage is found as

$$\frac{d\hat{v}_{dc}}{dt} = \begin{cases} \dfrac{\hat{i}_{dc} - i_{gl}}{C} & \left(\hat{v}_{dc} > 0\right) + (\hat{i}_{dc} > i_{gl}) \\[1.5em] -k\hat{v}_{dc} & \overline{\left(\hat{v}_{dc} > 0\right) + (\hat{i}_{dc} > i_{gl})} \end{cases} \tag{5.6.34}$$

The terms to the right in (5.6.33) and (5.6.34) are Boolean, and that the over-bar denotes logical complement.

5.6.6 Generator Circuit Breaker Control

The circuit breaker control is depicted in Fig. 5.6.2. The inputs to the control are the desired status of the breaker, o_{gcb}^* , the dc voltage, v_{dc} , the minimum dc voltage, $v_{dc,\min}$, the load

current, i_{gl}, and the fault current threshold, i_{glf}. The output of the control is the circuit breaker status, c_g.
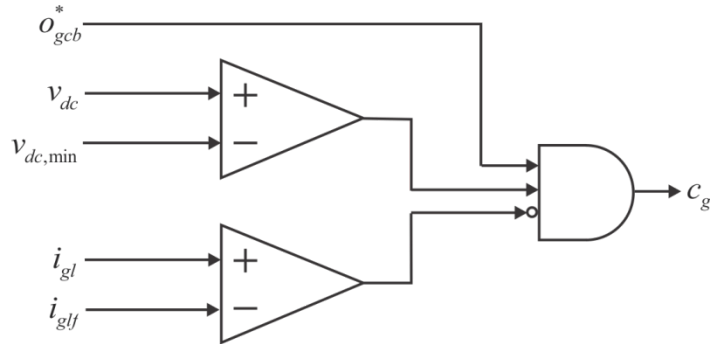
Fig. 5.6.2: DC Generator Circuit Breaker Control.

When a fault occurs the load current will rise above the fault current threshold causing the breaker status to go low and the breaker to open. In order to check if the fault is cleared, a low voltage supply is placed on the dc bus to trickle charge it. If there is no fault, then the dc voltage will rise above the minimum dc voltage value and, assuming the desired circuit breaker state is high, the circuit breaker will close. If the fault is still in place, the dc voltage will not rise and the circuit breaker will remain open.

Validation:
The generator rectifier model has been used extensively. It may be rigorously derived, and has been shown to accurately predict experimentally observed results. The main limitation is for very heavily loaded cases in which the thyristor conduction pattern changes.

References:
[5.6.1] Sudhoff, S.D.; Corzine, K. A.; Hegner, H.J.; Delisle, D.E., "Transient and dynamic average-value modeling of synchronous machine fed load-commutated converters," *Energy Conversion, IEEE Transactions on* , vol.11, no.3, pp.508,514, Sep 1996.

5.7 DC WRSM Exciter Model

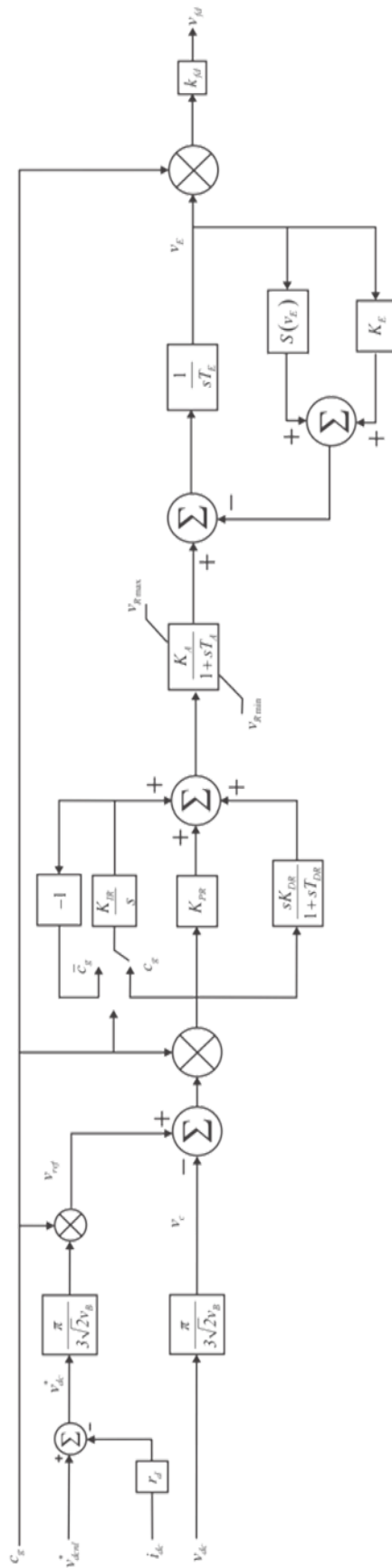The dc generator exciter is based upon IEEE AC8B [5.7.1] and is depicted in Fig. 5.7.1.

Fig. 5.7.1: DC Generator Exciter.

33

Inputs:

c_g Circuit breaker status (1 is closed, 0 is open)

i_{dc} The measured dc current (A)

v_{dc} The measured dc voltage (V)

Outputs:

v_{fd} The referred exciter voltage (V)

Parameters:

v_{dcnl}^* The no load dc voltage (V)

v_{rated} The rated dc link voltage (V)

v_B Base voltage (V)

r_d Droop resistance (Ω)

K_{PR} Automatic Voltage Regulator (AVR) proportional gain (pu)

K_{IR} AVR integral gain (pu)

K_{DR} AVR derivative gain (pu)

T_{DR} AVR derivative time constant (s)

K_A AVR power stage gain (pu)

T_A AVR power stage time constant (s)

$v_{R\max}$ AVR positive ceiling voltage (pu)

$v_{R\min}$ AVR negative ceiling voltage (pu)

T_E Exciter field time constant (s)

K_E Exciter field proportional gain (pu)

Interface Equations:
None

Model Equations:

      The droop resistance is found

$$r_d = \frac{v_{dcnl}^* - v_{dcfl}^*}{i_{dcfl}} \tag{5.7.1}$$

in which v_{dcfl}^* is the desired full load voltage and i_{dcfl} is the full load dc current.

      The reference voltage for the exciter, v_{ref}, is determined by converting the desired dc voltage, v_{dc}^*, to the rms line-line representation needed by the exciter. The desired dc voltage is obtained as the difference of the desired no load dc voltage and the dc current multiplied by r_d. The reference voltage is modulated by the circuit breaker status, c_g. The measured bus voltage for the exciter, v_C, is obtained as the rms line-line representation of the measured dc voltage.

The model equations for the exciter are not explicitly given here as they are readily formulated from Fig. 5.7.1.

The saturation block is defined as

$$S(v_E) = 1.0119 e^{0.875 v_E} \tag{5.7.2}$$

The integral term of the PI control is switched between either the error between the measured and reference voltages, or the negative of the integral term based upon the status of the circuit breaker. This winds down the integral term of the control if the circuit breaker opens due to a fault.

The referred field voltage is obtained from the per-unit field voltage v_E using

$$v_{fd} = c_g k_{fd} v_E \tag{5.7.3}$$

where k_{fd} is defined by (5.3.4).

Validation:

This is a behavioral model commonly used in the power engineering community to represent a rotating-rectifier type exciter and is discussed in [5.7.1].

References:

[5.7.1] L.M. Hajagos and M.J. Basler, "Changes to IEEE 421.5 recommended practice for excitation system models for power stability studies", IEEE/PES 2005 Meeting, San Francisco, CA.

5.8 Propulsion Drive Model

The propulsion drive consists of a dc link, an inverter, and a permanent magnet synchronous machine as depicted in Fig. 5.8.1. In ac applications, this drive modeled is used in conjunction with the rectifier model presented in the following section.

The dc link consists of a capacitor C_{dc} and a braking resistor r_{rb}. The inverter is an active current controlled inverter driving a slightly salient permanent magnet synchronous machine.
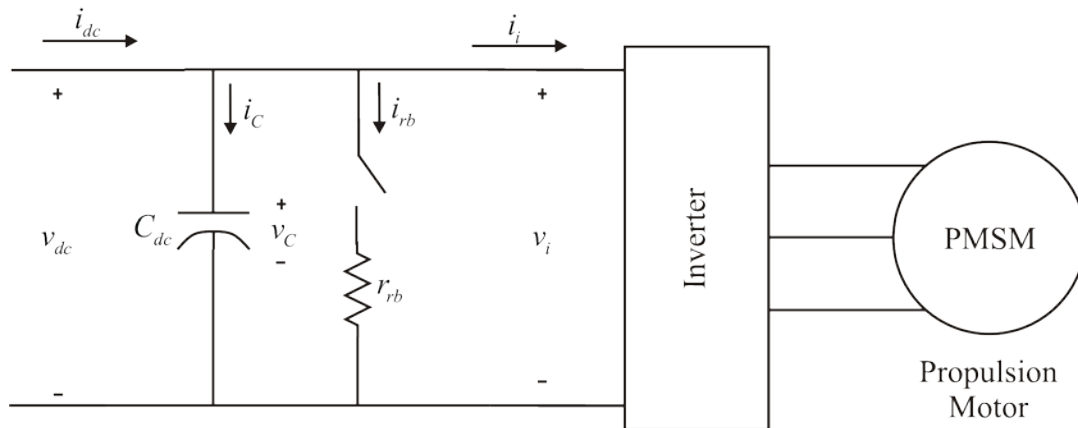

Fig. 5.8.1: DC Propulsion Drive.

The model structure is as follows

Inputs:

v_{dc} The dc bus voltage (V)

ω_{rm} The mechanical speed of the propulsion drive (rad/s)

o_{pd}^* The desired operational status of the drive

ω_{rm}^* The desired mechanical speed of the propulsion drive (rad/s)

$T_{L,\text{est}}$ The estimated load torque of the propulsion drive (Nm)

Outputs:

v_{qs} The *q*-axis voltage of the propulsion motor (V)

v_{ds} The *d*-axis voltage of the propulsion motor (V)

P_i The power drawn from the inverter (W)

i_{qs} The *q*-axis current into the propulsion motor (A)

i_{ds} The *d*-axis current into the propulsion motor (A)

T_e The output electrical torque of the propulsion motor (Nm)

Parameters:

P The number of poles in the PMAC

λ_m The flux linkage due to the permanent magnet (Vs)

L_q The *q*-axis inductance of the machine (H)

L_d The *d*-axis inductance of the machine (H)

r_s The stator resistance of the machine (Ω)

C_{dc} The dc link capacitance value (F)

r_{rb} The resistor brake resistance value (Ω)

K_p The speed control proportional gain $\left(\dfrac{\text{Nm}}{\text{rad/s}} \right)$

K_i The speed control integral gain $\left(\dfrac{\text{Nm}}{\text{rad}} \right)$

ω_{rmr} The rated mechanical speed of the drive (rad/s)

T_{mx} The maximum allowable commanded torque (Nm)

T_{mn} The minimum allowable commanded torque (Nm)

$\dot{T}_{emxi}$ The maximum rate of change in commanded torque (Nm/s)

$\dot{T}_{emni}$ The minimum rate of change in commanded torque (Nm/s)

τ_{nsc} The non-linear stabilizing control time constant (s)

v_{fmx} The maximum non-linear stabilizing control voltage (V)

v_{fmn} The minimum non-linear stabilizing control voltage (V)

n_{nsc} The order of the non-linear stabilizing control

Δv_i An allowed margin for error in the inverter voltage (V)

Interface Equations:

States:

v_c The dc link capacitor voltage (V)

Model Equations:

5.8.1   PMAC Motor and Drive Model

The propulsion motor is a slightly salient PMSM. The model for this machine is defined in [5.8.1] and outlined herein. First, the electrical speed of the machine is

$$\omega_r = \frac{P}{2}\omega_{rm} \tag{5.8.1}$$

where ω_{rm} is the mechanical speed of the machine, and P is the number of poles. The machine model is defined using a *qd0* framework in the rotor reference frame. The reduced-order voltage equations in the rotor reference frame are presented in *qd* form as

$$v_{qs}^r = r_s i_{qs}^r + \omega_r L_d i_{ds}^r + \omega_r \lambda_m \tag{5.8.2}$$

$$v_{ds}^r = r_s i_{ds}^r - \omega_r L_q i_{qs}^r \tag{5.8.3}$$

where r_s is the stator winding resistance, L_q and L_d are the *q* and *d* axis inductances, λ_m is the flux linkage due to the permanent magnet, and ω_r is the angular velocity of the rotor. The inverter considered is an active current controlled inverter and so the currents obtained can be assumed to be the desired currents. Therefore the *q* and *d* axis currents are obtained using

$$i_{qs}^r = \begin{cases} \dfrac{4T_e^*}{3P\lambda_m} & o_{pd} \\ 0 & \overline{o}_{pd} \end{cases} \tag{5.8.4}$$

$$i_{ds}^r = \begin{cases} 0 & \overline{o}_{pd} \text{ or } \left(v_{aiv} \geq v_{riv}\right) \\ \dfrac{-b_{fw} + \sqrt{b_{fw}^2 - 4a_{fw}c_{fw}}}{2a_{fw}} & o_{pd} \text{ and } \left(v_{aiv} < v_{riv}\right) \end{cases} \tag{5.8.5}$$

where o_{pd} is the operational status of the drive, v_{aiv} is the available inverter voltage, v_{riv} is the required inverter voltage, and a_{fw}, b_{fw}, and c_{fw} are defined as

$$a_{fw} = r_s^2 + \omega_r^2 L_d^2 \tag{5.8.6}$$

$$b_{fw} = 2(r_s i_{qs}^r + \omega_r \lambda_m)\omega_r L_d - 2r_s i_{qs}^r L_q \omega_r \tag{5.8.7}$$

37

$$c_{fw} = \frac{1}{3}(v_{ri}^2 - v_{aiv}^2)$$

(5.8.8)

The available inverter voltage is

$$v_{aiv} = v_i - \Delta v_i$$

(5.8.9)

where Δv_i represents an allowed margin. The required inverter voltage is

$$v_{riv} = \sqrt{3}\sqrt{(r_s i_{qs}^r + \omega_r \lambda_m)^2 + (\omega_r L_q i_{qs}^r)^2}$$

(5.8.10)

The inverter power is then found using

$$P_i = \frac{3}{2}\left(v_{qs}^r i_{qs}^r + v_{ds}^r i_{ds}^r\right)$$

(5.8.11)

and the inverter current is

$$i_i = \begin{cases} \dfrac{P_i}{v_i} & o_{pd} \\ 0 & \overline{o}_{pd} \end{cases}$$

(5.8.12)

5.8.2 DC Link and Resistor Brake

The dc link in the propulsion drive is depicted in Fig. 5.8.2. The dc link consists of a capacitor and the braking resistor.
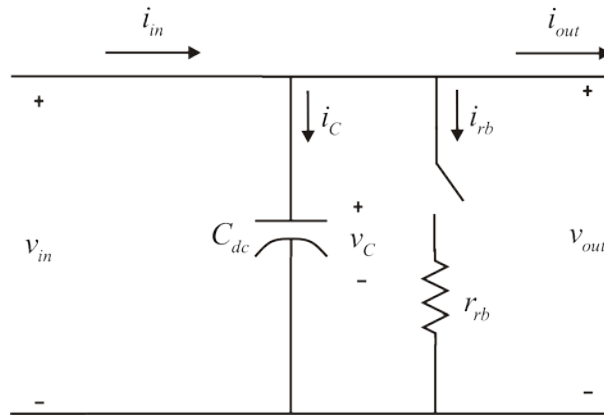

Fig. 5.8.2: DC Link.

The equations defining the dc link are

$$\frac{dv_c}{dt} = \frac{i_C}{C_{dc}}$$

(5.8.13)

38

$$i_{rb} = \begin{cases} 0 & o_{rb} = 0 \\ \dfrac{v_{out}}{r_{rb}} & o_{rb} = 1 \end{cases} \tag{5.8.14}$$

$$i_{in} = i_C + i_{rb} + i_{out} \tag{5.8.15}$$

where o_{rb} is the operational status of the resistor brake. The control for the resistor brake is depicted in Fig. 5.8.3. The output of the control, o_{rb}, is the operational status of the resistor brake and is determined by the level of the dc voltage at the input to the dc link. The threshold voltages for the resistor brake consist of an enable threshold, v_{rbe} and a disable threshold, v_{rbd}. The enable threshold, v_{rbe} is assumed to be greater than v_{rbd}. If the dc voltage is above v_{rbe}, the threshold for the brake to turn on, then o_{rb} is high, if the voltage goes below v_{rbd}, the voltage level to disable the resistive brake, o_{rb} goes low.
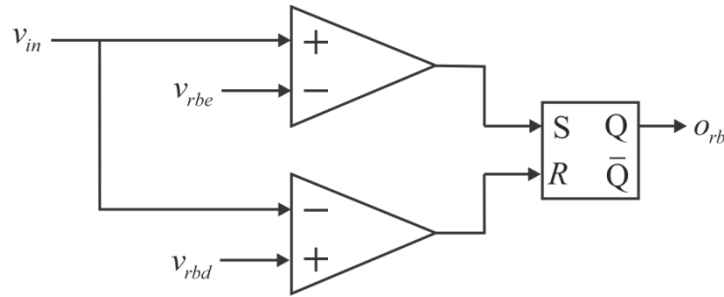
Fig. 5.8.3: Resistor Brake Control.

5.8.3 Propulsion Drive Control

The control for the propulsion drive is depicted in Fig. 5.8.4. The output of the control is T_e^*, the desired electrical torque for the propulsion motor. This torque value is obtained from a PI speed control followed by a slew rate limiter.

Fig. 5.8.4: Propulsion Control.
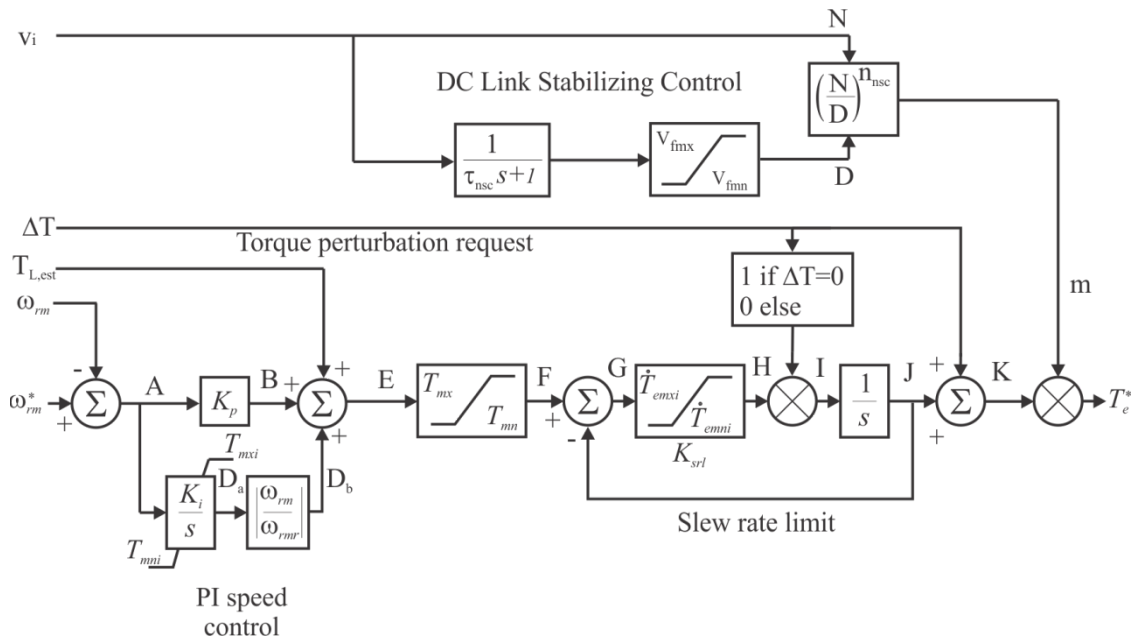
A torque perturbation request is facilitated and the dc link voltage stabilizing control is incorporated into the torque value that is subject to the operation state of the drive. The non-linear stabilizing control time constant is obtained using

$$\tau_{nsc} = 10\sqrt{\left(L_{dc} + 2L_c\right)C_{dc}} \tag{5.8.16}$$

5.8.4 Propulsion Drive Supervisory Control
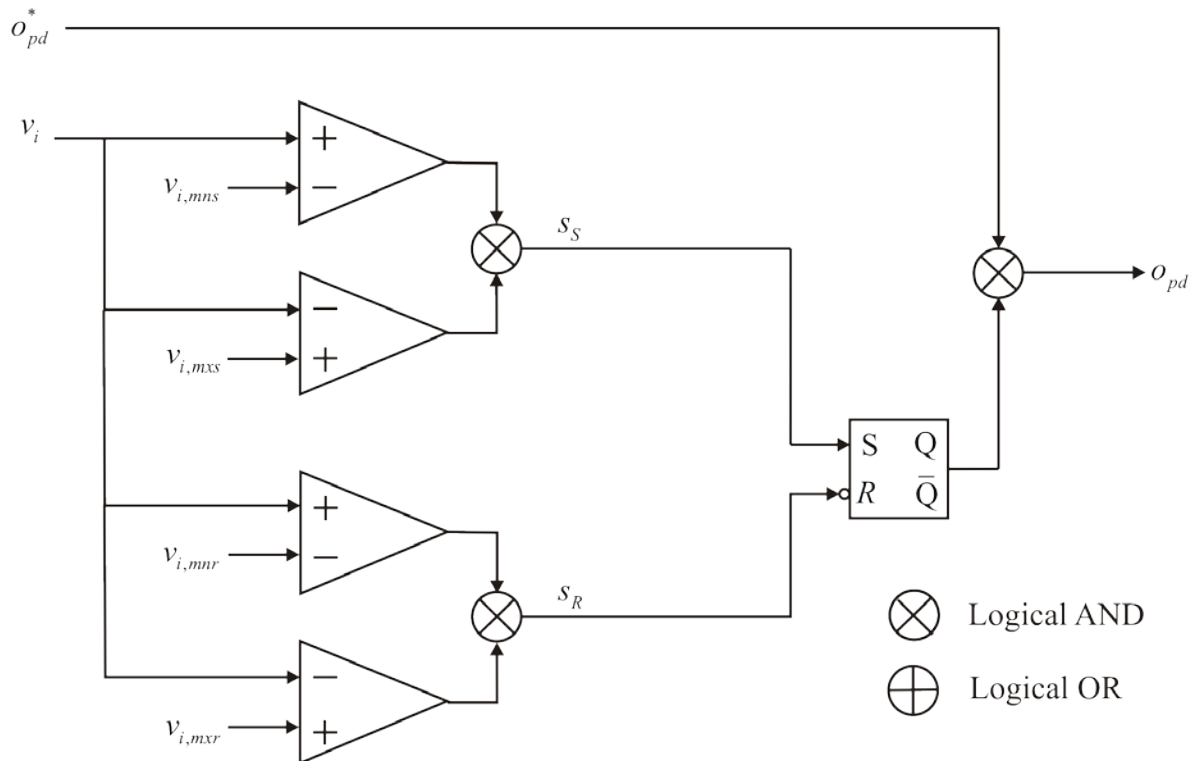
Fig. 5.8.5: DC Propulsion Supervisory Control.

The supervisory control for the propulsion drive is shown in Fig. 5.8.5. The output of the control is o_{pd}, the operational state of the drive. The inputs are o_{pd}^*, startup, and v_i, the desired operational state of the drive, whether the drive is in startup mode, and the dc voltage at the terminals of the inverter respectively. The operational state is determined by the inverter voltage being within startup limits during startup and within running limits during operation along with the desired operational status of the drive.

Validation:

With respect to the propulsion drive model, the propulsion motor and inverter module models are simple, well-established, and observed to be reasonably accurate. The control models again represent an intended control, and so must be judged in terms of effectiveness rather than in terms of accuracy.

References:
[5.8.1] P. Krause, O. Wasynczuk, S. Sudhoff, and S. Pekarek, "Analysis of Electric Machinery and Drive Systems," 3rd Edition, New York: John Wiley and Sons/IEEE Press, 2013.

5.9 Propulsion Drive Rectifier

For ac applications, in addition to the components listed in the previous section, the propulsion drive also includes a rectifier model. The propulsion drive rectifier model is depicted in Fig. 5.9.1. Like the propulsion machine model, the transformer rectifier model utilizes the qd framework and is presented in detail in [5.9.1].
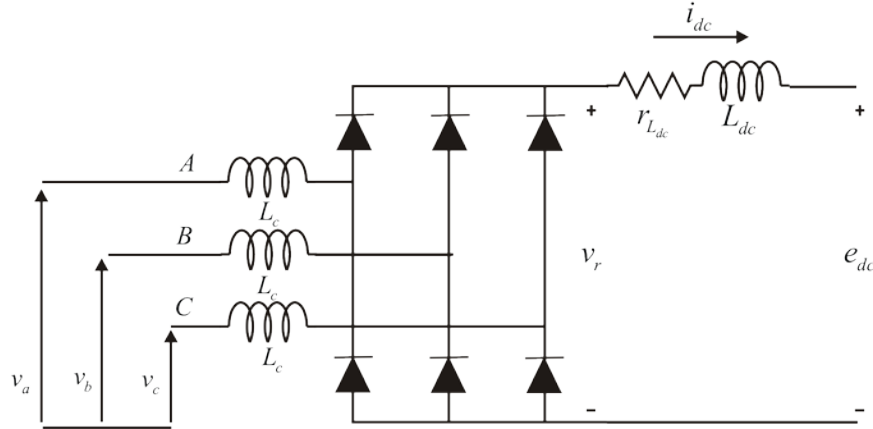
Fig. 5.9.1: Propulsion Drive Transformer Rectifier.

The structure of the ac propulsion load model is as follows.

Inputs:

v_q^a The q-axis voltage in the arbitrary reference frame (V)

v_d^a The d-axis voltage in the arbitrary reference frame (V)

Outputs:

i_q^a The q-axis current in the arbitrary reference frame (A)

i_q^a The d-axis current in the arbitrary reference frame (A)

Parameters:

L_c The commutating inductance of the rectifier (H)

L_{dc} The inductance of the dc link inductor (H)

r_{Ldc} The resistance of the dc link inductor (Ω)

Interface Equations:
None

States:

$\hat{i}_{dc}$ The average dc link inductor current (A)

Model Equations:

The model inputs are the q and d axis voltages of the ac input in the arbitrary reference frame and the outputs are the q and d axis currents in that same reference frame. To facilitate this, the frame-to-frame transformation

$$\mathbf{f}_{qd}^{g} = {}^{a}\mathbf{K}^{g}\mathbf{f}_{qd}^{a} \tag{5.9.1}$$

is used where

$$
{}^{a}\mathbf{K}^{g} = \begin{bmatrix} \cos\left(\theta_{ga}\right) & -\sin\left(\theta_{ga}\right) \\ \sin\left(\theta_{ga}\right) & \cos\left(\theta_{ga}\right) \end{bmatrix} \tag{5.9.2}
$$

and where 'g' denotes a generator reference frame wherein the q-axis voltage is positive and the d-axis voltage is zero. Applying (5.9.2) with

$$\theta_{ga} = -\text{angle}\left(v_{q}^{a} - jv_{d}^{a}\right) \tag{5.9.3}$$

yields

$$v_{q}^{g} = \sqrt{2}E \tag{5.9.4}$$

and

$$v_{d}^{g} = 0 \tag{5.9.5}$$

where

$$E = \frac{1}{\sqrt{2}}\sqrt{v_{q}^{a2} + v_{d}^{a2}} \tag{5.9.6}$$

In (5.9.3) and (5.9.6), v_{q}^{a} and v_{d}^{a} are the q and d axis voltages to the left of the ac side inductor L_{c} in Fig. 5.9.1. The average dc voltage to the right of the rectifier is defined as

$$\hat{v}_{r} = \frac{3\sqrt{6}}{\pi}E\cos\left(\alpha\right) - \frac{3}{\pi}L_{C}\omega_{g}\hat{i}_{dc} - 2L_{c}\frac{d\hat{i}_{dc}}{dt} \tag{5.9.7}$$

where α is the firing delay angle. This average dc voltage can be related to e_{dc} by

$$\hat{v}_{r} = r_{Ldc}\hat{i}_{dc} + L_{dc}\frac{d\hat{i}_{dc}}{dt} + e_{dc} \tag{5.9.8}$$

Therefore

$$p\hat{i}_{dc} = \frac{\dfrac{3\sqrt{6}}{\pi}E\cos\left(\alpha\right) - \left(r_{Ldc} + \dfrac{3}{\pi}L_{c}\omega_{g}\right)\hat{i}_{dc} - e_{dc}}{L_{dc} + 2L_{c}} \tag{5.9.9}$$

The derivative of the average dc current is expressed

$$\tag{5.9.10}$$

43

$$\frac{d\hat{i}_{dc}}{dt} = \begin{cases} p\hat{i}_{dc} & \text{f} \\ -k\hat{i}_{dc} & \text{\=f} \end{cases}$$

where f is

$$f = \left(\hat{i}_{dc} \geq 0\right) \cup \left(p\hat{i}_{dc} > 0\right) \tag{5.9.11}$$

and k is a constant.

The commutation angle is determined using the following. First, assuming a firing delay angle of zero,

$$\alpha_s = 0 \tag{5.9.12}$$

The commutation angle is found using

$$\mu_s = -\alpha_s + \text{acos}\left(\cos(\alpha_s) - \frac{2L_c\omega_g\hat{i}_{dc}}{\sqrt{6}E} \right) \tag{5.9.13}$$

This expression is only valid if several conditions are met. First,

$$\left| \cos(\alpha_s) - \frac{2L_c\omega_e\hat{i}_{dc}}{\sqrt{6}E} \right| \leq 1 \tag{5.9.14}$$

The second and third conditions are that $\mu_s \leq \frac{\pi}{3}$ and that $\mu_s + \alpha_s \leq \pi$. If these conditions are met, then the firing delay angle and commutation angle are

$$\alpha = \alpha_s \tag{5.9.15}$$

and

$$\mu = \mu_s \tag{5.9.16}$$

Otherwise the firing delay angle and commutation angle are taken to be

$$\alpha = \frac{\pi}{3} - \text{acos}\left(\text{bound}\left(-1, 1, \frac{2L_c\omega_g\hat{i}_{dc}}{\sqrt{6}E} \right) \right) \tag{5.9.17}$$

and

$$\mu = \frac{\pi}{3} \tag{5.9.18}$$

The expressions (5.9.17) and (5.9.18) assume 3-3 mode rectifier operation.

The first step in the calculation of the q and d axis currents is the calculation of the commutation interval currents defined as

$$\tag{5.9.19}$$

44

$$\hat{i}^g_{qg,com} = \frac{2\sqrt{3}}{\pi}\hat{i}_{dc}\left[\sin\left(\mu+\alpha-\frac{5\pi}{6}\right)-\sin\left(\alpha-\frac{5\pi}{6}\right)\right]$$

$$+\frac{3}{\pi}\frac{\sqrt{2}E}{L_c\omega_g}\cos(\alpha)[\cos(\mu+\alpha)-\cos(\alpha)]$$

$$+\frac{1}{4}\frac{3}{\pi}\frac{\sqrt{2}E}{L_c\omega_g}[\cos(2\alpha)-\cos(2\alpha+2\mu)]$$

$$\hat{i}^g_{dg,com} = \frac{2\sqrt{3}}{\pi}\hat{i}_{dc}\left[-\cos\left(\mu+\alpha-\frac{5\pi}{6}\right)+\cos\left(\alpha-\frac{5\pi}{6}\right)\right]$$

$$+\frac{3}{\pi}\frac{\sqrt{2}E}{L_c\omega_g}\cos(\alpha)[\sin(\mu+\alpha)-\sin(\alpha)] \tag{5.9.20}$$

$$+\frac{1}{4}\frac{3}{\pi}\frac{\sqrt{2}E}{L_c\omega_g}[\sin(2\alpha)-\sin(2\alpha+2\mu)]-\frac{3}{\pi}\frac{\sqrt{2}E}{L_c\omega_g}\frac{1}{2}\mu$$

The conduction interval ac currents are found using

$$\hat{i}^g_{qg,cond} = \frac{2\sqrt{3}}{\pi}\hat{i}_{dc}\left[\sin\left(\alpha+\frac{7\pi}{6}\right)-\sin\left(\alpha+\mu+\frac{5\pi}{6}\right)\right] \tag{5.9.21}$$

$$\hat{i}^g_{dg,cond} = \frac{2\sqrt{3}}{\pi}\hat{i}_{dc}\left[-\cos\left(\alpha+\frac{7\pi}{6}\right)+\cos\left(\alpha+\mu+\frac{5\pi}{6}\right)\right] \tag{5.9.22}$$

The ac currents are then the sum of the conduction and commutation interval ac currents.

$$\hat{i}_{qg} = \hat{i}_{q,com}+\hat{i}_{q,cond} \tag{5.9.23}$$

$$\hat{i}_{dg} = \hat{i}_{d,com}+\hat{i}_{d,cond} \tag{5.9.24}$$

These currents are then transformed back to the arbitrary reference frame using the inverse of the reference frame transformation (5.9.2). Namely, the currents into the rectifier are given by

$$\hat{i}^a_q = \hat{i}^g_q\cos\left(\theta_{ga}\right)+\hat{i}^g_d\sin\left(\theta_{ga}\right) \tag{5.9.25}$$

$$\hat{i}^a_d = -\hat{i}^g_q\sin\left(\theta_{ga}\right)+\hat{i}^g_d\cos\left(\theta_{ga}\right) \tag{5.9.26}$$

Validation:

This is also a well-established model. The chief limitations that will arise are that the accuracy of the model deteriorates if the ac bus voltages become highly disturbed. Further, the rectifier model is only valid in the 2-3 and 3-3 modes of operation. Finally, if the dc link or ac side inductances saturate, the accuracy of the model will decrease.

45

References:
[5.9.1] P. Krause, O. Wasynczuk, S. Sudhoff, and S. Pekarek, "Analysis of Electric Machinery and Drive Systems," 3rd Edition, New York: John Wiley and Sons/IEEE Press, 2013.
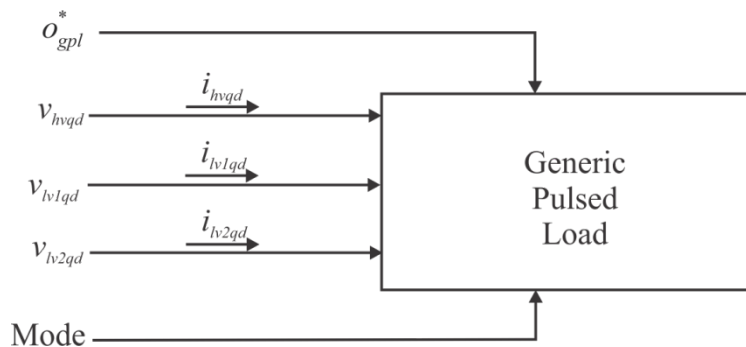
5.10 Generic Pulsed Load

The generic pulsed load exists in two contexts, dc and ac. The dc generic pulsed load is depicted in Fig. 5.10.1. The load is fed by two voltage level busses. A low voltage bus is used for the control and ancillaries and a high voltage bus is used for the bulk power. There are two low voltage busses present for redundancy purposes. The low voltage busses are ac busses and the high voltage bus is dc. There are two modes considered in the pulsed load, standby and operational.
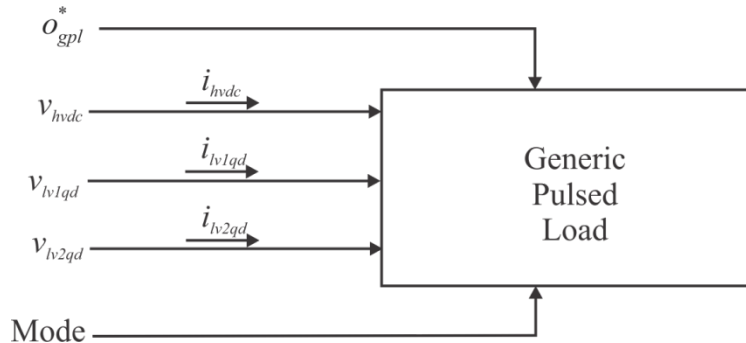
Fig. 5.10.1: DC Generic Pulsed Load.

The ac generic pulsed load is depicted in Fig. 5.10.2. The load is once again fed by two voltage level busses, a high voltage bus and a low voltage bus. However, in this case the high voltage bus is an ac bus and is represented in *qd* form. The other inputs to the load are the same as those for the dc generic pulsed load.

Fig. 5.10.2: AC Generic Pulsed Load.

The model structure for the generic pulsed load is as follows.

Inputs:

o_{gpl}^* The desired operational status of the load

v_{hvXX} The high voltage bus where XX is either *dc* or *qd* (V)

v_{lv1qd} The *qd* representation of the primary low voltage bus (V)

v_{lv2qd} The *qd* representation of the secondary low voltage bus (V)

Outputs:

i_{hvXX} The current on the high voltage bus where XX is either *dc* or *qd* (A)

i_{lv1qd} The ac current on the primary low voltage bus (A)

i_{lv2qd} The ac current on the secondary low voltage bus (A)

Parameters:

$v_{hv,mns}$ The minimum voltage to start for the high voltage bus (V)

$v_{hv,mxs}$ The maximum voltage to start for the high voltage bus (V)

$v_{hv,mnr}$ The minimum voltage to run for the high voltage bus (V)

$v_{hv,mxr}$ The maximum voltage to run for the high voltage bus (V)

$v_{lv1,mns}$ The minimum voltage to start for the primary bus (V)

$v_{lv1,mxs}$ The maximum voltage to start for the primary bus (V)

$v_{lv2,mns}$ The minimum voltage to start for the secondary bus (V)

$v_{lv2,mxs}$ The maximum voltage to start for the secondary bus (V)

$v_{lv1,mnr}$ The minimum voltage to run for the primary bus (V)

$v_{lv1,mxr}$ The maximum voltage to run for the primary bus (V)

$v_{lv2,mnr}$ The minimum voltage to run for the secondary bus (V)

$v_{lv2,mxr}$ The maximum voltage to run for the secondary bus (V)

P_{hvS} The high voltage standby mode real power level (W)

Q_{hvS} The high voltage standby mode reactive power level (W)

P_{lvS} The low voltage standby mode real power level (W)

Q_{lvS} The low voltage standby mode reactive power level (W)

P_{hvO} The high voltage operation mode real power level (W)

Q_{hvO} The high voltage operation mode reactive power level (W)

P_{lvO} The high voltage operation mode real power level (W)

Q_{lvO} The high voltage operation mode reactive power level (W)

Interface Equations:
None

States:
None

Model Equations:
None

5.10.1 DC Operation

For the dc application of the generic pulsed load, the high voltage bus is a dc bus where v_{hvdc} is the dc voltage on the bus and i_{hvdc} is the dc current being drawn from the bus. The low voltage bus is represented in *qd* form as

$$\boldsymbol{v}_{lvXqd} = \begin{bmatrix} v_{lvXq} \\ v_{lvXd} \end{bmatrix}$$ (5.10.1)

and

$$\boldsymbol{i}_{lvXqd} = \begin{bmatrix} i_{lvXq} \\ i_{lvXd} \end{bmatrix}$$ (5.10.2)

where *X* can be either *1* or *2* depending on which low voltage bus being referred to.

The dc power for each bus is defined in Table 1. The values for these power levels are listed in the Nominal System Parameters section of the document.

Table 1: DC Operation

Power	Mode	
	Standby	**Operational**
P_{hv}	P_{hvS}	P_{hvO}
P_{lv}	P_{lvS}	P_{lvO}
Q_{lv}	Q_{lvS}	Q_{lvO}

5.10.2 AC Operation

In the ac application of the generic pulsed load the high voltage bus is an ac bus as well as the low voltage busses. In this case the high voltage bus, like the low voltage bus, is represented in *qd* form as

$$v_{hvqd} = \begin{bmatrix} v_{hvq} \\ v_{hvd} \end{bmatrix}$$ (5.10.3)

and

$$i_{hvqd} = \begin{bmatrix} i_{hvq} \\ i_{hvd} \end{bmatrix}$$ (5.10.4)

The ac application of the generic pulsed load is similar to the dc operation, but also includes the apparent power levels for the two modes for each bus. These power levels are listed in Table 2. The values for these power levels are listed in the Nominal System Parameters section of the document.

48

	Mode	
Power	**Standby**	**Operational**
P_{hv}	P_{hvS}	P_{hvO}
Q_{hv}	Q_{hvS}	Q_{hvO}
P_{lv}	P_{lvS}	P_{lvO}
Q_{lv}	Q_{lvS}	Q_{lvO}

5.10.3 Supervisory Control

The supervisory control for the generic pulsed load is shown in Fig. 5.10.3. The inputs to the control are the desired operational status of the pulsed load, o_{pd}^*, the measured high voltage bus level, v_{hvm}, the measured first low voltage bus level, v_{lv1m}, and the measured second low voltage bus level, v_{lv2m}. The measured low voltage bus levels are obtained by

$$v_{lvXm} = \frac{1}{\sqrt{6}} \sqrt{v_{lvXq}^2 + v_{lvXd}^2} \qquad (5.10.5)$$

where *X* can be either *1* or *2* depending on which low voltage bus being referred to. The dc application high voltage measurement is equal to v_{hvdc}, and the ac application high voltage bus measurement is obtained as

$$v_{hvm} = \frac{1}{\sqrt{6}} \sqrt{v_{hvq}^2 + v_{hvd}^2} \qquad (5.10.6)$$
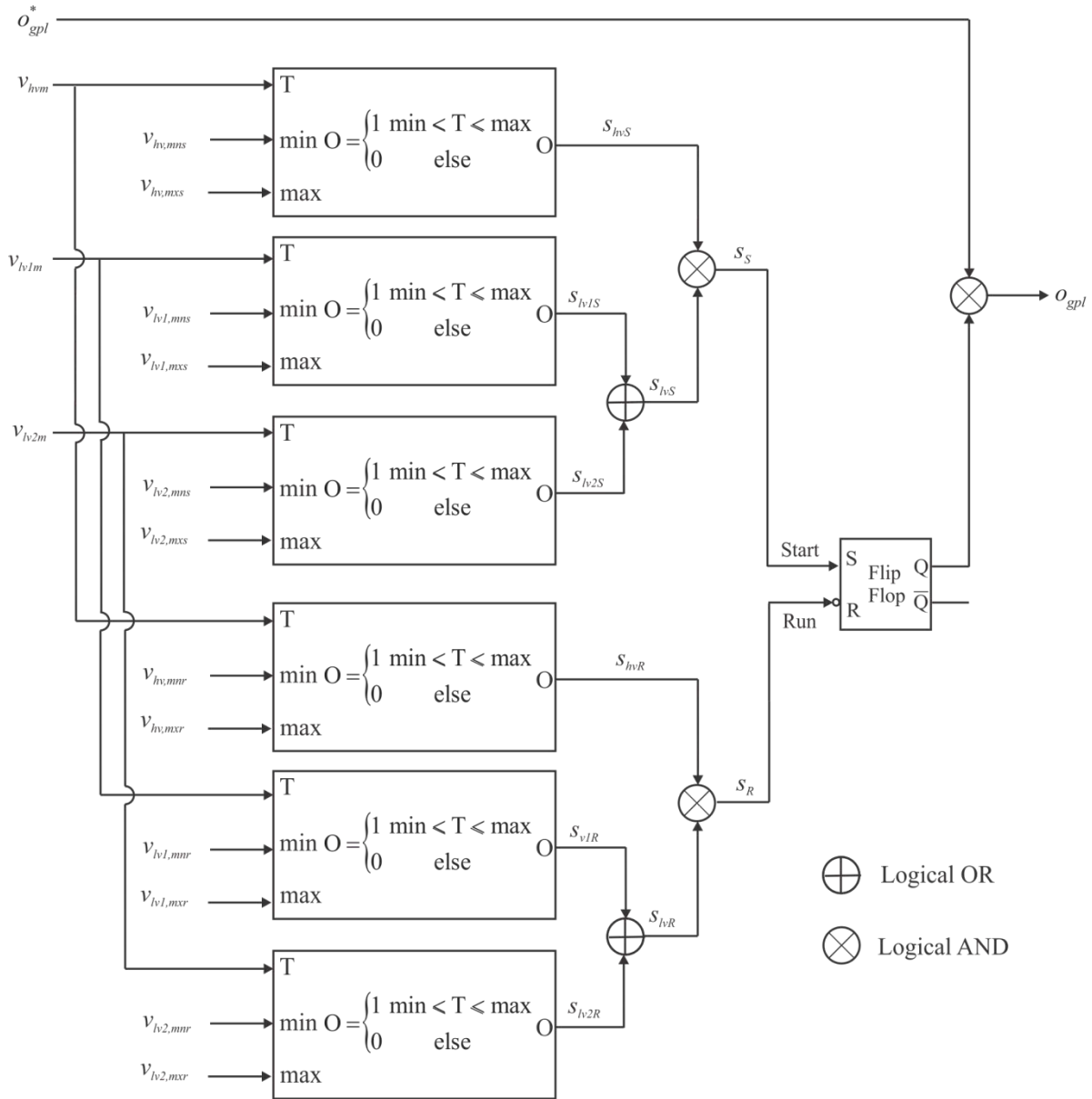
Fig. 5.10.3: GPL Supervisory Control.

There are two situations governed by the control. The first is during the startup condition and the second is during a running condition. These two conditions have different minimum and maximum voltage level requirements with the startup condition being the more stringent of the two. The output of the control is the operational state of the generic pulsed load and is dependent on the voltage levels for the three busses being within the limits for either the startup or running condition. The startup intermediate control variables s_{hvS}, s_{lv1S}, and s_{lv2S} are true if the corresponding bus voltages are within their ranges governed by the appropriate min and max voltage levels. One of the low voltage busses must be within the required range and the high voltage bus must be within the required range in order for the operational state of the drive to be enabled. This same control scheme is used for the running condition which if not satisfied resets the operational state of the pulsed load.

50

5.10.4 Model Outputs

The outputs of the generic pulsed load are the currents for the three busses. For the dc application where the high voltage bus is dc, the high voltage bus current, i_{hv}, is

$$i_{hv} = \begin{cases} 0 & o_{gpl} = 0 \\ \dfrac{P_{hvS}}{v_{hv}} & o_{gpl} = 1, \text{mode} = \text{standby} \\ \dfrac{P_{hvO}}{v_{hv}} & o_{gpl} = 1, \text{mode} = \text{operational} \end{cases} \tag{5.10.7}$$

In the ac application of the pulsed load, the high voltage bus is an ac bus and therefore, the q-axis current of the high voltage bus is

$$i_{hvq} = \begin{cases} 0 & o_{gpl} = 0 \\ \dfrac{v_{hvq}P_{hvS} - v_{hvd}Q_{hvS}}{\frac{3}{2}\left(v_{hvq}^2 + v_{hvd}^2\right)} & o_{gpl} = 1, \text{mode} = \text{standby} \\ \dfrac{v_{hvq}P_{hvO} - v_{hvd}Q_{hvO}}{\frac{3}{2}\left(v_{hvq}^2 + v_{hvd}^2\right)} & o_{gpl} = 1, \text{mode} = \text{operation} \end{cases} \tag{5.10.8}$$

and the d-axis current on the high voltage bus is

$$i_{hvd} = \begin{cases} 0 & o_{gpl} = 0 \\ \dfrac{v_{hvd}P_{hvS} + v_{hvq}Q_{hvS}}{\frac{3}{2}\left(v_{lv1q}^2 + v_{lv1d}^2\right)} & o_{gpl} = 1, \text{mode} = \text{standby} \\ \dfrac{v_{hvd}P_{hvO} + v_{hvq}Q_{hvO}}{\frac{3}{2}\left(v_{hvq}^2 + v_{hvd}^2\right)} & o_{gpl} = 1, \text{mode} = \text{operation} \end{cases} \tag{5.10.9}$$

Regardless of dc or ac application of the generic pulsed load, the low voltage bus is ac and the q-axis current on the first low voltage bus is

$$
i_{lv1q} = \begin{cases} 0 & o_{gpl} = 0 \text{ or } s_{lv1R}=0 \\[4ex] \dfrac{v_{lv1q}P_{lvS} - v_{lv1d}Q_{lvS}}{\dfrac{3}{2}\left(v_{lv1q}^2 + v_{lv1d}^2\right)} & o_{gpl} = 1 \text{ and mode = standby and } s_{lv1R}=1 \\[4ex] \dfrac{v_{lv1q}P_{lvO} - v_{lv1d}Q_{lvO}}{\dfrac{3}{2}\left(v_{lv1q}^2 + v_{lv1d}^2\right)} & o_{gpl} = 1 \text{ and mode = operation and } s_{lv1R}=1 \end{cases} \tag{5.10.10}
$$

The *q*-axis current on the second low voltage bus is

$$
i_{lv2q} = \begin{cases} 0 & o_{gpl} = 0 \text{ or } s_{lv1R}=1 \text{ or } s_{lv2R}=0 \\[4ex] \dfrac{v_{lv2q}P_{lvS} - v_{lv2d}Q_{lvS}}{\dfrac{3}{2}\left(v_{lv2q}^2 + v_{lv2d}^2\right)} & o_{gpl} = 1 \text{ and mode = standby and } s_{lv1R}=0 \text{ and } s_{lv2R}=1 \\[4ex] \dfrac{v_{lv2q}P_{lvO} - v_{lv2d}Q_{lvO}}{\dfrac{3}{2}\left(v_{lv2q}^2 + v_{lv2d}^2\right)} & o_{gpl} = 1 \text{ and mode = operation and } s_{lv1R}=0 \text{ and } s_{lv2R}=1 \end{cases} \tag{5.10.11}
$$

The *d*-axis current on the first low voltage bus is

$$
i_{lv1d} = \begin{cases} 0 & o_{gpl} = 0 \text{ or } s_{lv1R}=0 \\[4ex] \dfrac{v_{lv1d}P_{lvS} + v_{lv1q}Q_{lvS}}{\dfrac{3}{2}\left(v_{lv1q}^2 + v_{lv1d}^2\right)} & o_{gpl} = 1 \text{ and mode = standby and } s_{lv1R}=1 \\[4ex] \dfrac{v_{lv1d}P_{lvO} + v_{lv1q}Q_{lvO}}{\dfrac{3}{2}\left(v_{lv1q}^2 + v_{lv1d}^2\right)} & o_{gpl} = 1 \text{ and mode = operation and } s_{lv1R}=1 \end{cases} \tag{5.10.12}
$$

The d-axis current on the second low voltage bus is

$$i_{lv2d} = \begin{cases} 0 & o_{gpl} = 0 \text{ and } s_{lv1R} = 1 \text{ and } s_{lv2R} = 0 \\[2ex] \dfrac{v_{lv2d}P_{lvS} + v_{lv2q}Q_{lvS}}{\dfrac{3}{2}\left(v_{lv2q}^2 + v_{lv2d}^2\right)} & o_{gpl} = 1 \text{ and mode} = \text{standby and } s_{lv1R} = 0 \text{ and } s_{lv2R} = 1 \\[3ex] \dfrac{v_{lv2d}P_{lvO} + v_{lv2q}Q_{lvO}}{\dfrac{3}{2}\left(v_{lv2q}^2 + v_{lv2d}^2\right)} & o_{gpl} = 1 \text{ and mode} = \text{operation and } s_{lv1R} = 0 \text{ and } s_{lv2R} = 1 \end{cases} \quad (5.10.13)$$

If both of the low voltage busses are present and both i_{hv} and i_{hv} are high, then the first bus is selected as the bus used to power the control and ancillaries of the GPL.

Validation:
The model is an abstraction of the requirement of a generic pulsed load (or constant power load) which consumes the desired power, but no internal dynamics are represented.

References:
None

5.11 Generic Hydrodynamic Load

The generic hydrodynamic load model is defined in [5.12.1-5.12.3] and outlined herein. The model structure is as follows.

Inputs:
ω_{prop} Propeller angular frequency (rad/s)

Outputs:
T_{prop} Counter torque exerted on shaft (Nm)
V_{ship} Ship velocity (m/s)

Parameters:
ρ	Density of salt water (kg/m^3)
D	Propeller diameter (m)
η_r	Relative rotational efficiency (pu)
V_a	Propeller speed of advance (m/s)
υ	Modified advanced coefficient (pu)
$C_Q(\upsilon)$	Open water propeller torque coefficient function
$C\tau(\upsilon)$	Open water propeller thrust coefficient function
$w_T(V_{ship})$	Taylor wake fraction
T_d	Thrust deduction factor

m_{ship} Mass of ship (kg)

$F_{drag}\left(V_{ship}\right)$ Hydrodynamic resistance (N vs knots)

Interface equation:
None

States:
V_{ship} Ship velocity (m/s)

Model Equations:
         The model definition for the generic hydrodynamic load is given in [5.12.1] and outlined herein. First, the propeller speed of advance is found utilizing the Taylor Wake fraction as

$$V_a = V_{ship}\left(1 - \mathrm{w_T}\left(V_{ship}\right)\right) \tag{5.11.1}$$

Next, the thrust exerted on the ship is found using

$$F_{ship} = \mathrm{C_\tau}(\upsilon)\rho D^2 (V_a^{\;2} + (nD)^2)(1 - T_d) \tag{5.11.2}$$

where

$$n = \frac{\omega_{prop}}{2\pi} \tag{5.11.3}$$

and

$$\upsilon = \frac{nD}{\sqrt{V_a^{\;2} + (nD)^2}} \tag{5.11.4}$$

Next, the derivative of ship speed is found using

$$\frac{dV_{ship}}{dt} = \frac{1}{m_{ship}}\left[F_{ship1} + F_{ship2} - F_{drag}\left(V_{ship}\right)\right] \tag{5.11.5}$$

where F_{ship1} and F_{ship2} are the thrust exerted on the ship by propellers one and two. Finally, the counter torque on the propeller shaft is found using

$$T_{prop} = \mathrm{C_Q}(\upsilon)\rho\left(\frac{D^3}{\eta_r}\right)(V_a^{\;2} + (nD)^2) \tag{5.11.6}$$

Validation:
         The hydrodynamic represented here is general and valid for a given set of torque and thrust coefficients, and ship resistance, which all depend on various factors including propeller type, ship hull form, and operating conditions such as sea state conditions, and the presence of cavitation, for example. Further discussion and analysis of ship propulsion can be found in [5.12.4] and [5.12.5].

References:
[5.12.1] E. J. Lecourt, Jr., "Using Simulation To Determine the Maneuvering Performance of the WAGB-20," Naval Engineer's Journal, January 1998, pp. 171-188.
[5.12.2] Syntek, "DD(X) Notional Baseline Modeling and Simulation Development Report," Internal Report, August 2003.
[5.12.3] Robert F. Roddy, David E. Hess, and Will Faler, "Neural Network Predictions of the 4-Quadrant Wageningen Propeller Series, NSWCCD-50-TR-2006/004, Naval Surface Warfare Center, Carderock Division, West Bethesda, MD, April 2006.
[5.12.4] K.J. Rawson, E.C. Tupper, "Basic Ship Theory," Longman Scientific and Technical, Volume 2 , 1994.
[5.12.5] V. Bertram, "Practical Ship Hydrodynamics," Elsevier Ltd, 2nd Edition, 2012.

5.12 Line Models

5.12.1 DC Line

This section sets forth descriptions of the ac and dc line models. The dc line is a resistive line and the model structure is as follows.

Inputs:

$v_{dc,x}$ The dc voltage at bus x (V)

$v_{dc,y}$ The dc voltage at bus y (V)

Outputs:

$i_{dc,xy}$ The dc current through the line from bus x to bus y (A)

Interface equation:

$$v_{dc,y} = v_{dc,x} - r_{dc}i_{dc,xy} \tag{5.12.1}$$

States:
None

Model Equation:

$$i_{dc,xy} = \frac{v_{dc,x} - v_{dc,y}}{r_{dc}} \tag{5.12.2}$$

Validation:
The chief sources of inaccuracy in this model are that temperature dependence and line inductance are neglected. This will cause the line model to tend to overestimate fault currents.

References:
None

5.12.2 AC Line

The ac line is an RL line and the model structure is as follows.

Inputs:

$\mathbf{v}^e_{qd,x}$ The vector of *q*- and *d*-axis voltages ($v^e_{q,x}$ and $v^e_{d,x}$) at bus *x* of the line in the synchronous ref. frame (V)

$\mathbf{v}^e_{qd,y}$ The vector of *q*- and *d*-axis voltages ($v^e_{q,y}$ and $v^e_{d,y}$) at bus *y* of the line in the synchronous ref. frame (V)

ω_e The radian frequency of the synchronous reference frame (rad/s)

Outputs:

$\mathbf{i}^e_{qd,xy}$ The *q*- and *d*-axis currents ($i^e_{q,xy}$ and $i^e_{d,xy}$) through the line from bus *x* to bus *y* in the synchronous ref. frame (A)

Interface equation:

$$\mathbf{v}^e_{qd,y} = \mathbf{v}^e_{qd,x} - \mathbf{Z}^e_{qd}\mathbf{i}^e_{qd,xy} \tag{5.12.3}$$

where

$$\mathbf{Z}^e_{qd} = \begin{bmatrix} r & \omega_e L \\ -\omega_e L & r \end{bmatrix} \tag{5.12.4}$$

States:
None

Model Equations:

$$\mathbf{i}^e_{qd,xy} = \left(\mathbf{Z}^e_{qd}\right)^{-1}\left(\mathbf{v}^e_{qd,x} - \mathbf{v}^e_{qd,y}\right) \tag{5.12.5}$$

Validation:

This line model neglects temperature dependence. The line inductance is included, but only in a steady-state sense. Thus, fault current will tend to be overestimated. . In addition, it is assumed that the line is balanced and symmetrical.

References:
None

5.13 AC Circuit Breaker Model

The ac circuit breaker model represents the opening and closing of the breaker as a change in resistance. This is done in such a way as to avoid discontinuities. The breaker either opens due to the measured current being greater than a threshold indicating a fault, or if the desired circuit breaker status (o^*_{acb}) is open. If the breaker trips due to an over-current, the desired

circuit breaker status must be set low for a certain period of time in order to reset the circuit breaker. The model structure for the ac circuit breaker is as follows.

Inputs:

o_{acb}^* The desired circuit breaker status

I_s The measured current used to indicate a fault (A)

Outputs:

R_{cb} The resistance of the circuit breaker (Ω)

Parameters:

I_t The threshold current that defines a fault condition (A)

R_{closed} The closed resistance of the circuit breaker (Ω)

R_{open} The open resistance of the circuit breaker (Ω)

τ_o The time constant associated with a manual change of operational status (s)

τ_f The time constant associated with a fault detection (s)

Interface equation:
None

States:

o_{acb} The operational status of the circuit breaker

F The fault status of the circuit breaker

Model Equations:

There are two values in the control that define whether the breaker is in operation and if there is a fault condition. The operational status of the breaker is represented by o and the fault status of the breaker is represented by F. The governing equations for these two control values are

$$\dot{o}_{acb} = \begin{cases} 1 & o_{acb}^* = 1 \text{ and } o_{acb} \leq 1 \\ -1 & o_{acb}^* = 0 \text{ and } o_{acb} \geq 0 \\ 0 & \left(o_{acb}^* = 0 \text{ and } o_{acb} < 0\right) or \left(o_{acb}^* = 1 \text{ and } o_{acb} > 1\right) \end{cases} \tag{5.13.1}$$

and

$$\dot{F} = \begin{cases} 1 & \begin{aligned} &\left(I_s > I_t \text{ and } F < 1\right) \text{ or} \\ &\left(o_{acb} > 0 \text{ and } I_s < I_t \text{ and } \left(F > 0 \text{ and } F < 1\right)\right) \end{aligned} \\ -1 & \left(o_{acb} \leq 0 \text{ and } I_s < I_t \text{ and } F > 0\right) \\ 0 & \begin{aligned} &\left(I_s > I_t \text{ and } F \geq 1\right) \text{ or} \\ &\left(I_s < I_t \text{ and } F \leq 1\right) \text{ or} \\ &\left(o_{acb} > 0 \text{ and } I_s < I_t \text{ and } F \geq 1\right) \end{aligned} \end{cases} \tag{5.13.2}$$

The derivatives of the control signals are then calculated as

$$\frac{do_{acb}}{dt} = \frac{1}{\tau_o} \dot{o}_{acb}$$
(5.13.3)

$$\frac{dF}{dt} = \frac{1}{\tau_F} \dot{F}$$
(5.13.4)

The status of the circuit breaker (open/closed) is then governed by

$$c = \min(o_{acb}, 1 - F)$$
(5.13.5)

and the resistance of the circuit breaker is

$$R = 10^{\log(R_{\max}) - c\left(\log(R_{\max}) - \log(R_{\min})\right)}$$
(5.13.6)

Validation:

It must be recognized that this model is completely behavioral in nature. Functionally, it will operate as a circuit breaker and interrupt a fault current and be re-closable. However, the dynamics of the circuit breaker are not based on physics and so the model does not correctly portray the short-time scale behavior of circuit breaker operation.

References:
None

5.14 Transformer

The *q* and *d*-axis equivalent circuits for the transformer model are depicted in Fig. 5.14.1 and Fig. 5.14.2.
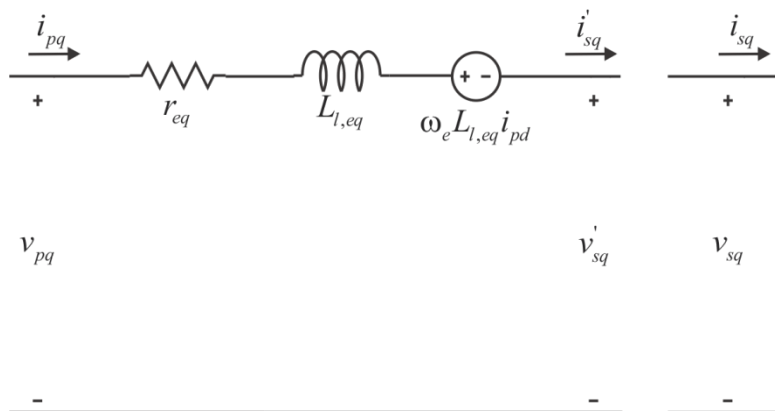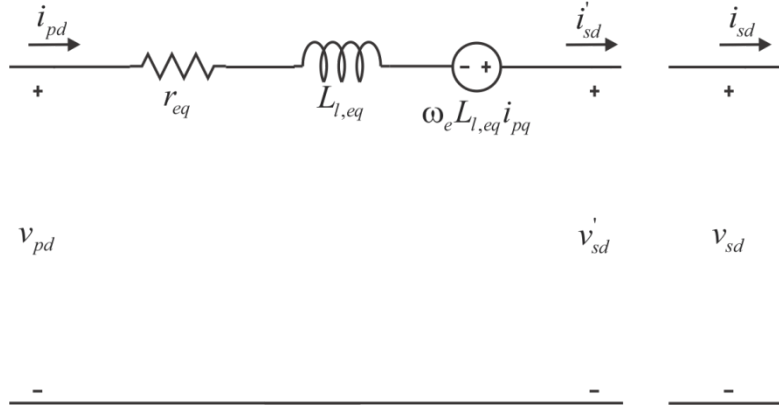

Fig. 5.14.1: Transformer *Q*-axis Equivalent Circuit.

Fig. 5.14.2: Transformer *D*-axis Equivalent Circuit.

The equivalent resistance (r_{eq}) and inductance (L_{eq}) are found using

$$r_{eq} = r_p + r_s'$$ (5.14.1)

$$L_{l,eq} = L_{lp} + L_{ls}'$$ (5.14.2)

The model structure is as follows.

Inputs:

$v_{p,qd}$ The primary side voltage in the *qd* reference frame (V)

$i_{s,qd}$ The secondary side current in the *qd* reference frame (A)

ω_e The electrical speed of the synchronous reference frame (rad/s)

Outputs:

$v_{s,qd}$ The secondary side voltage in the *qd* reference frame (V)

$i_{p,qd}$ The primary side current in the *qd* reference frame (A)

Parameters:

r_p The primary side winding resistance (Ω)

r_s' The secondary side winding resistance referred to the primary side (Ω)

L_{lp} The primary side winding leakage inductance (H)

L_{ls}' The secondary side winding leakage inductance referred to the primary side (H)

N_p The number of turns on the primary winding

N_s The number of turns on the secondary winding

Interface Equations:

$$v_{pq} = r_{eq}i_{pq} + \omega_e L_{l,eq}i_{pd} + v_{sq}'$$ (5.14.3)

$$v_{pd} = r_{eq}i_{pd} - \omega_e L_{l,eq}i_{pq} + v_{sd}'$$ (5.14.4)

59

States:
None

Model Equations:
    The relationship between the referred and non-referred quantities is

$$v'_{sX} = \frac{N_p}{N_s} v_{sX} \tag{5.14.5}$$

and

$$i'_{sX} = \frac{N_s}{N_p} i_{sX} \tag{5.14.6}$$

where X can either be *q* or *d*.

$$i'_{sX} = i_{pX} \tag{5.14.7}$$

Lastly, the resistance and inductance are referred using

$$r'_s = \left(\frac{N_p}{N_s}\right)^2 r_s \tag{5.14.8}$$

and

$$L'_{ls} = \left(\frac{N_p}{N_s}\right)^2 L_{ls} \tag{5.14.9}$$

Validation:
    The model described assumes a balanced three phase transformer. The magnetizing inductance is assumed to be infinite, and the leakage saturation and temperature effects are ignored. Since this is a reduced-order model, initial fault currents will tend to be over-predicted.

References:
None

5.15 Zonal Active Rectifier

    The Zonal Active Rectifier is depicted in Fig. 5.15.1.
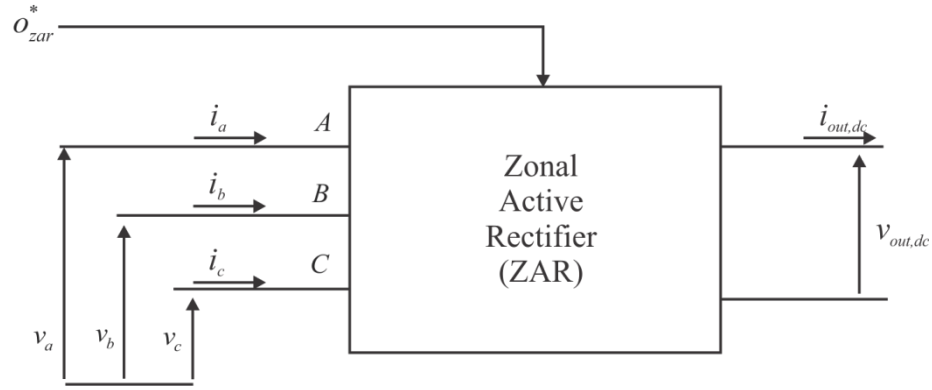
Fig. 5.15.1: Zonal Active Rectifier.

The model structure for the Zonal Active Rectifier is as follows.

Inputs:

$v_{in,qd}$ The ac side voltage in the *qd* reference frame (V)

$i_{out,dc}$ The dc output current (A)

o_{zar}^* The desired status of the component

Outputs:

$i_{in,qd}$ The ac side current in the *qd* reference frame (A)

$v_{out,dc}$ The dc output voltage (V)

Parameters:

r_d The droop resistance (Ω)

v_{out}^* The desired no load output voltage (V)

i_t The fault current threshold (A)

i_f The peak fault current (A)

Interface Equations:
None

States:
None

Model Equations:

  The supervisory control for the Zonal Active Rectifier is shown in Fig. 5.15.2. The inputs to the control are the measured voltage level of the bus and the desired operational status of the load, o_{zar}^*. The output of the supervisory control is the operational state of the load, o_{zar}. The supervisory control categorizes the bus voltage into two categories. The first category relates to being appropriate to start and the second relates to whether the bus voltage is appropriate to continue running. These two conditions have different minimum and maximum voltages level requirements with the startup condition being the more stringent of the two. The output of the control is the operational state of the load, o_{zar}^*, and is dependent upon the voltage

levels of the buss being within the limits for either the startup or running condition. The intermediate control variables S_S and S_R are true if the bus voltage is within the ranges governed by the appropriate min and max voltage levels for component start or run. If the bus is within its required voltage range then the flip-flop is not reset. If it is out of range then the flip-flop is reset.
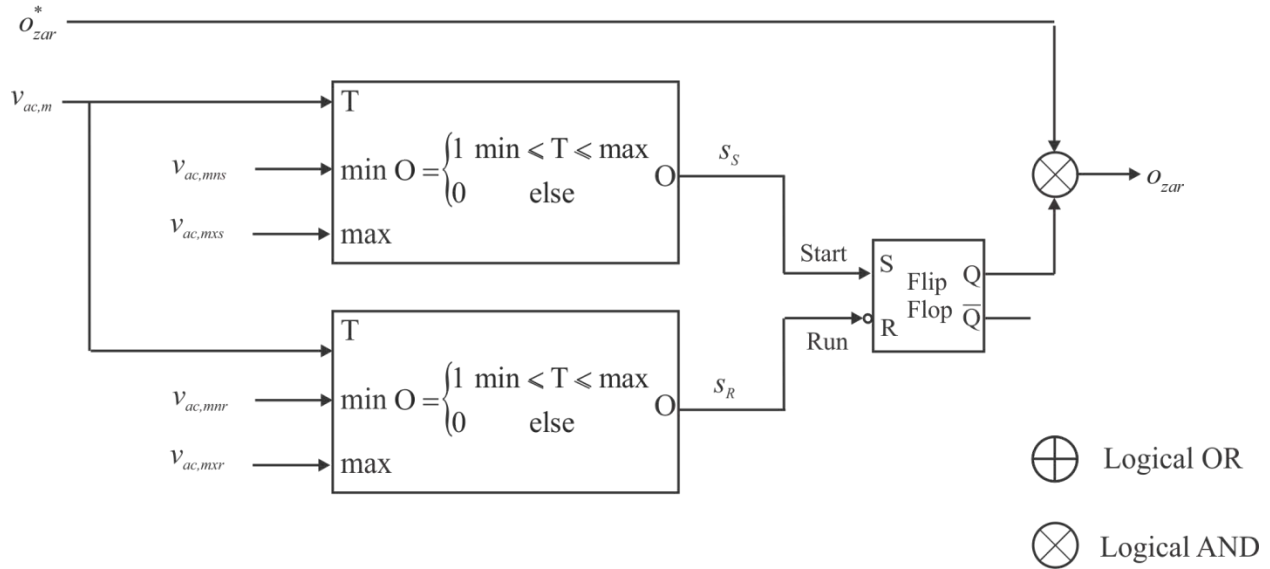
Fig. 5.15.2: Zonal Active Rectifier Supervisory Control.

The dc output voltage of the rectifier as a function of output current is depicted in Fig. 5.15.3.
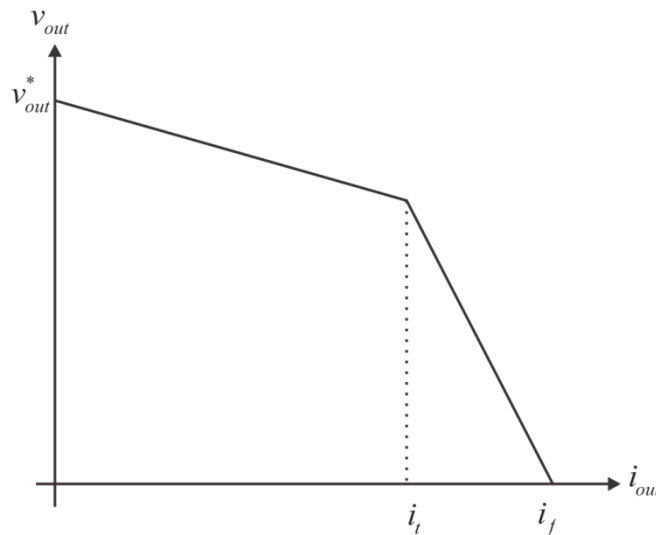
Fig. 5.15.3: Zonal Active Rectifier Output Voltage.

The output voltage is therefore expressed

$$v_{out} = \begin{cases} 0 & o_{zar} = 0 \text{ or } i_{out} > i_f \\ v^*_{out} - r_d i_{out} & o_{zar} = 1 \text{ and } i_{out} < i_t \\ m i_{out} + c & o_{zar} = 1 \text{ and } i_{out} \geq i_t \end{cases} \tag{5.15.1}$$

where

$$m = \frac{r_d i_t - v^*_{out}}{i_f - i_t} \tag{5.15.2}$$

and

$$c = \frac{\left(v^*_{out} - r_d i_t\right) i_f}{i_f - i_t} \tag{5.15.3}$$

The output power is found using

$$P_{out} = v_{out} i_{out} \tag{5.15.4}$$

and the input power is found using

$$P_{in} = \frac{P_{out}}{\eta_{inc}} + P_{nl} \tag{5.15.5}$$

where

$$\eta_{inc} = \frac{\Delta P_{out}}{\Delta P_{in}} \tag{5.15.6}$$

is the incremental efficiency. The q and d-axis currents can then be calculated using

$$i_q = \frac{\frac{2}{3} P_{in} v_q}{v_q^2 + v_d^2} \tag{5.15.7}$$

and

$$i_d = \frac{\frac{2}{3} P_{in} v_d}{v_q^2 + v_d^2} \tag{5.15.8}$$

Validation:
    The behavior of this component is based on what is possible in terms of power balance. It is an abstraction of a desired component performance.

References:
None

5.16 Type 1 DC Load

The Type 1 dc load is depicted in Fig. 5.16.1 and is a resistive load fed by one of two busses. The first input bus is the primary power source and the second bus supplies backup power.
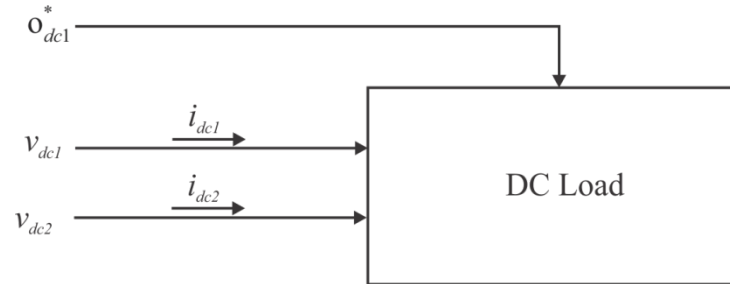

Fig. 5.16.1: Zonal DC Load.

The model structure is defined as follows.

Inputs:

o_{dc1}^* The desired operational status of the load

v_{dc1} The dc voltage on the primary bus (V)

v_{dc2} The dc voltage on the secondary bus (V)

Outputs:

i_{dc1} The dc current on the primary bus (A)

i_{dc2} The dc current on the secondary bus (A)

Parameters:

$v_{lv1,mns}$ The minimum voltage to start for the primary bus (V)

$v_{lv1,mxs}$ The maximum voltage to start for the primary bus (V)

$v_{lv2,mns}$ The minimum voltage to start for the secondary bus (V)

$v_{lv2,mxs}$ The maximum voltage to start for the secondary bus (V)

$v_{lv1,mnr}$ The minimum voltage to run for the primary bus (V)

$v_{lv1,mxr}$ The maximum voltage to run for the primary bus (V)

$v_{lv2,mnr}$ The minimum voltage to run for the secondary bus (V)

$v_{lv2,mxr}$ The maximum voltage to run for the secondary bus (V)

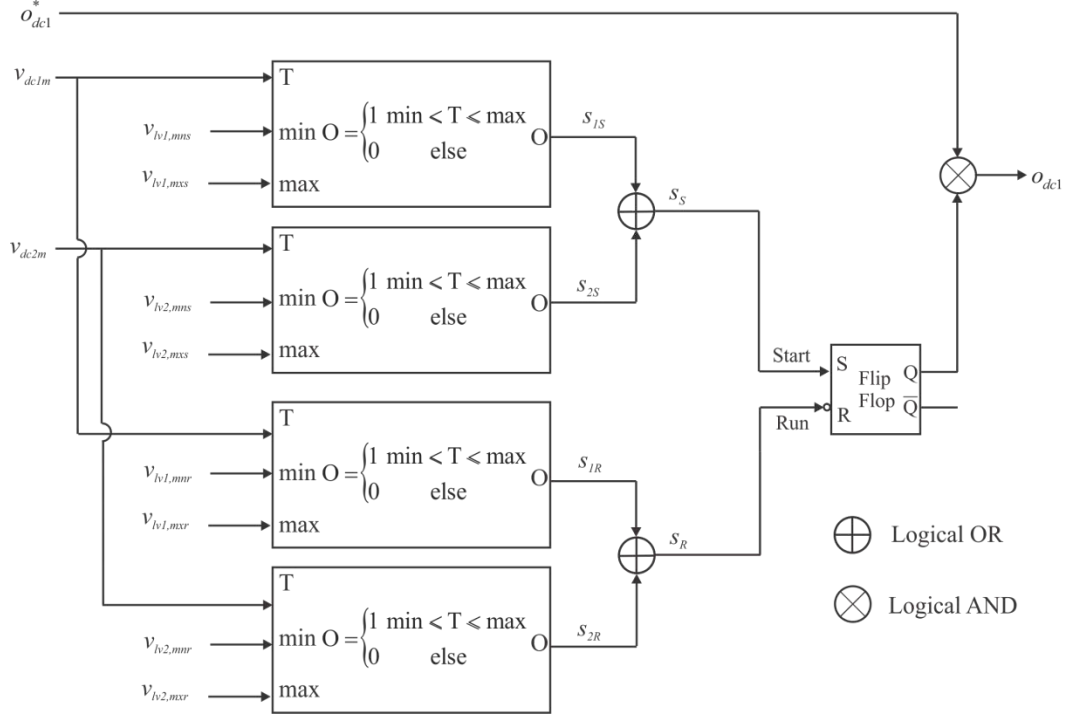r_{dc} The resistance of the dc load (Ω)

Interface Equations:
None

States:
None

Model Equations:

The supervisory control for the load is depicted in Fig. 5.16.2. The inputs to the supervisory control are the measured dc voltages on each of the two busses, v_{dc1m} and v_{dc2m}, and the desired operational status of the load, o_{dc1}^*.

Fig. 5.16.2: Zonal DC Load Supervisory Control.

The supervisory control categorizes each bus voltage into two categories. The first category relates to being appropriate to start and the second relates to whether the bus voltages are appropriate to continue running. These two conditions have different minimum and maximum voltages level requirements with the startup condition being the more stringent of the two. The output of the control is the operational state of the load, o_{dc1}^*, and is dependent upon the voltage levels for each of the busses being within the limits for either the startup or running condition. The intermediate control variables s_{1S} and s_{2S} are true if the corresponding bus voltages are within their ranges governed by the appropriate min and max voltage levels for component start. One bus being within the required range makes the set input of the flip-flop to true. The intermediate control variables s_{1R} and s_{1R} are true if the corresponding bus voltages are within the range governed by the appropriate min and max voltage levels to run. If either of the two busses is within its required voltage range then the flip-flop is not reset. If they both are out of range then the flip-flop is reset.

The output of the dc load model are the two load currents, i_{dc1} and i_{dc2}, which are given by

$$i_{dc1} = \begin{cases} 0 & o_{dc1} = 0 \text{ or } s_{1R} = 0 \\ \dfrac{v_{dc1}}{r_{dc}} & o_{dc1} = 1 \text{ and } s_{1R} = 1 \end{cases} \tag{5.16.1}$$

$$i_{dc2} = \begin{cases} 0 & o_{dc1} = 0 \text{ or } s_{2R} = 0 \\ \dfrac{v_{dc2}}{r_{dc}} & o_{dc1} = 1 \text{ and } s_{1R} = 0 \end{cases} \tag{5.16.2}$$

Validation:

The behavior of this component is based on what is possible in terms of power balance. It is an abstraction of a desired component performance.

References:
None

5.17 Type 2 DC Load

The type 2 dc load is the same configuration as the Type 1 dc load depicted in Fig. 5.16.1, but represents a constant power load. The model structure for this load is identical to that of the Type 1 dc load. The supervisory control for the load is identical to that of the Type 1 dc load depicted in Fig. 5.16.2 with the output being o_{dc2} instead of o_{dc1}.

The outputs of the Type 2 dc load model are the two load currents, i_{dc1} and i_{dc2}, which are given by

$$i_{dc1} = \begin{cases} 0 & o_{dc2} = 0 \text{ or } s_{1R} = 0 \\ \dfrac{P_{dc}}{v_{dc1}} & o_{dc2} = 1 \text{ and } s_{1R} = 1 \end{cases} \tag{5.17.1}$$

$$i_{dc2} = \begin{cases} 0 & o_{dc2} = 0 \text{ or } s_{2R} = 0 \\ \dfrac{P_{dc}}{v_{dc2}} & o_{dc2} = 1 \text{ and } s_{1R} = 0 \end{cases} \tag{5.17.2}$$

5.18 AC Load

The ac load is an RL load fed by two ac busses and is depicted in Fig. 5.18.1. The first input bus is the primary power source and the second bus supplies backup power.
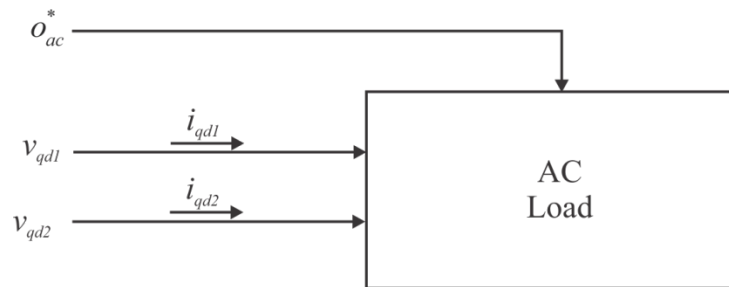
Fig. 5.18.1: Zonal AC Load.

The model structure is defined as follows.

Inputs:

o_{ac}^* The desired operational status of the load

v_{qd1} The ac voltage on the primary bus (V)

v_{qd2} The ac voltage on the secondary bus (V)

ω_e The electrical speed of the synchronous reference frame (rad/s)

Outputs:

i_{qd1} The ac current on the primary bus (A)

i_{qd2} The ac current on the secondary bus (A)

Parameters:

$v_{ac1,mns}$ The minimum voltage to start for the primary bus (V)

$v_{ac1,mxs}$ The maximum voltage to start for the primary bus (V)

$v_{ac2,mns}$ The minimum voltage to start for the secondary bus (V)

$v_{ac2,mxs}$ The maximum voltage to start for the secondary bus (V)

$v_{ac1,mnr}$ The minimum voltage to run for the primary bus (V)

$v_{ac1,mxr}$ The maximum voltage to run for the primary bus (V)

$v_{ac2,mnr}$ The minimum voltage to run for the secondary bus (V)

$v_{ac2,mxr}$ The maximum voltage to run for the secondary bus (V)

r_{ac} The resistance of the ac load (Ω)

L_{ac} The inductance of the ac load (Ω)
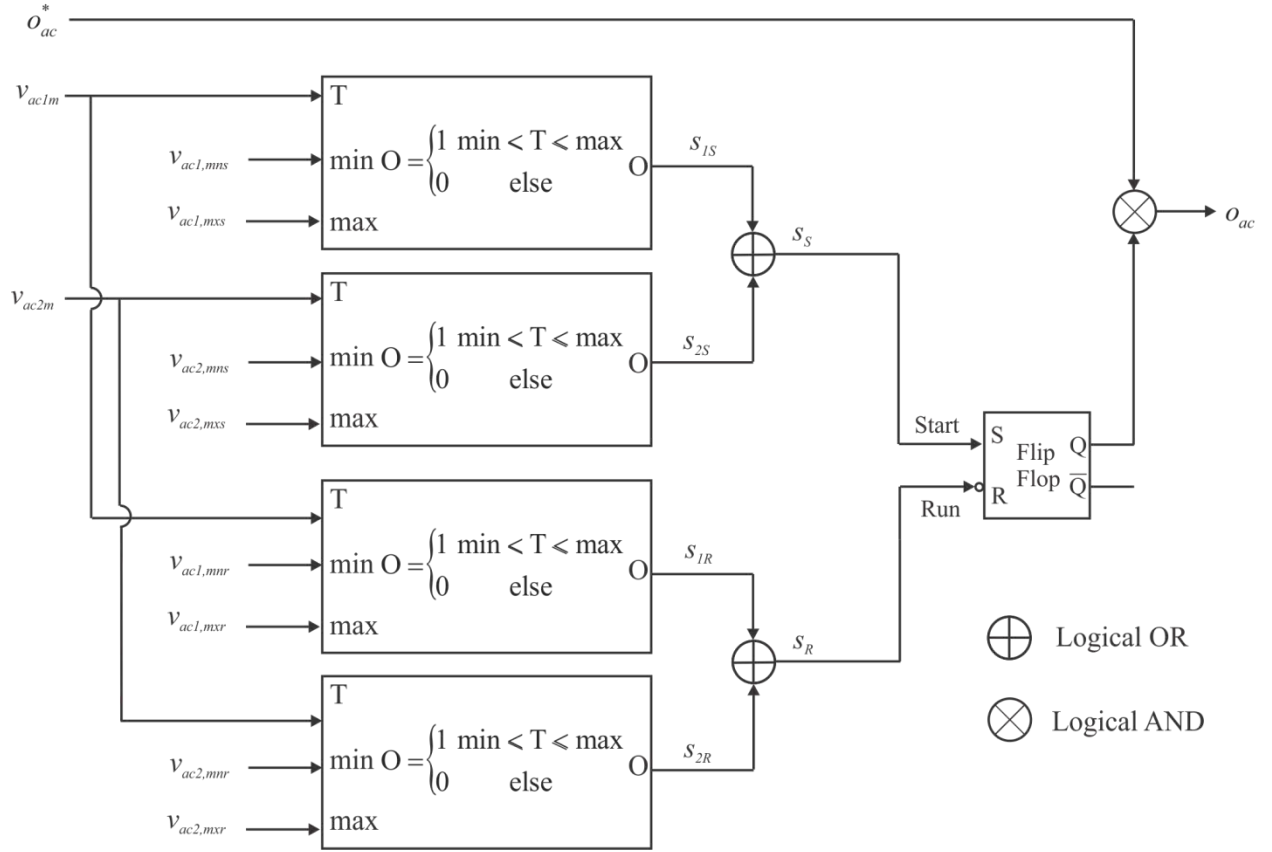
Interface Equations:
None

States:
None

Model Equations:

       The supervisory control for the ac load is depicted in Fig. 5.18.2. The inputs to the control are the measured voltage levels for each of the busses and the desired operational status of the load, o_{ac}^*. The output of the supervisory control is the operational state of the load, o_{ac}.

Fig. 5.18.2: Zonal AC Load Supervisory Control.

The measured voltage levels for the two busses are found using

$$v_{acXm} = \frac{1}{\sqrt{6}} \sqrt{v_{qX}^2 + v_{dX}^2} \tag{5.18.1}$$

where *X* can either be 1 or 2.

The supervisory control categorizes each bus voltage into two categories. The first category relates to being appropriate to start and the second relates to whether the bus voltages are appropriate to continue running. These two conditions have different minimum and maximum voltages level requirements with the startup condition being the more stringent of the two. The output of the control is the operational state of the load, o_{ac}^*, and is dependent upon the voltage levels for each of the busses being within the limits for either the startup or running condition. The intermediate control variables s_{1S} and s_{2S} are true if the corresponding bus voltages are within their ranges governed by the appropriate min and max voltage levels for component start. One bus being within the required range makes the set input of the flip-flop to true. The intermediate control variables s_{1R} and s_{1R} are true if the corresponding bus voltages are within the range governed by the appropriate min and max voltage levels to run. If either of the two busses is within its required voltage range then the flip-flop is not reset. If they both are out of range then the flip-flop is reset.

The model outputs for the ac load are the *q* and *d* axis currents for each of the busses, i_{q1}, i_{d1}, i_{q2} and i_{d2}, which are computed as

$$i_{q1} = \begin{cases} 0 & o_{ac} = 0 \text{ or } s_{ac1R} = 0 \\ \dfrac{r_{ac}v_{q1} - \omega L_{ac}v_{d1}}{r_{ac}^2 + \omega^2 L_{ac}^2} & o_{ac} = 1 \text{ and } s_{ac1R} = 1 \end{cases} \tag{5.18.2}$$

$$i_{d1} = \begin{cases} 0 & o_{ac} = 0 \text{ or } s_{ac1R} = 0 \\ \dfrac{r_{ac}v_{d1} + \omega L_{ac}v_{q1}}{r_{ac}^2 + \omega^2 L_{ac}^2} & o_{ac} = 1 \text{ and } s_{ac1R} = 1 \end{cases} \tag{5.18.3}$$

$$i_{q2} = \begin{cases} 0 & o_{ac} = 0 \text{ or } s_{ac2R} = 0 \\ \dfrac{r_{ac}v_{q2} - \omega L_{ac}v_{d2}}{r_{ac}^2 + \omega^2 L_{ac}^2} & o_{ac} = 1 \text{ and } s_{ac1R} = 0 \end{cases} \tag{5.18.4}$$

$$i_{d2} = \begin{cases} 0 & o_{ac} = 0 \text{ or } s_{ac2R} = 0 \\ \dfrac{r_{ac}v_{d2} + \omega L_{ac}v_{q2}}{r_{ac}^2 + \omega^2 L_{ac}^2} & o_{ac} = 1 \text{ and } s_{ac1R} = 0 \end{cases} \tag{5.18.5}$$

Validation:
   This component model is an exact steady-state model of a balanced RL load, neglecting temperature variations. It does not include dynamics.

References:
None

5.19 Isolated DC-DC Converter

   The IDCDC converter considered herein is an isolated, peak-current controlled, uni-directional DC-DC converter [5.21.1]. The topology is shown in Fig. 5.19.1. The control of the DC-DC converter is shown in Fig. 5.19.2. A simplified equivalent circuit used to derive the average value model (AVM) is seen in Fig. 5.19.3.
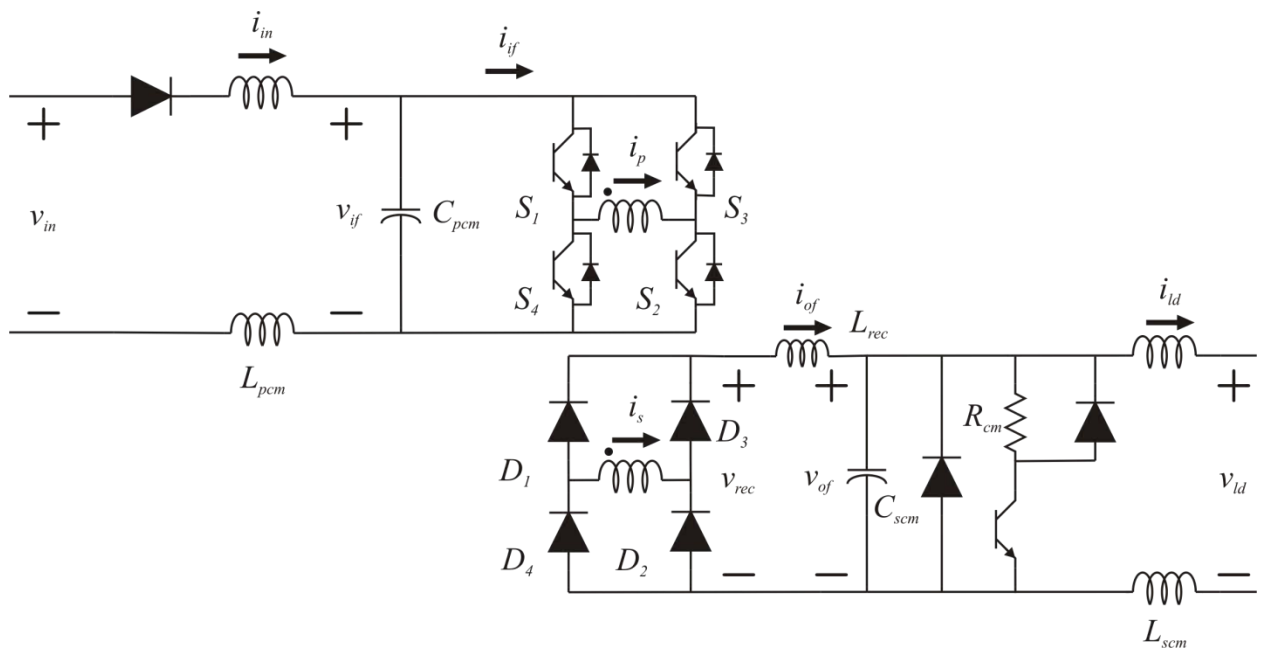
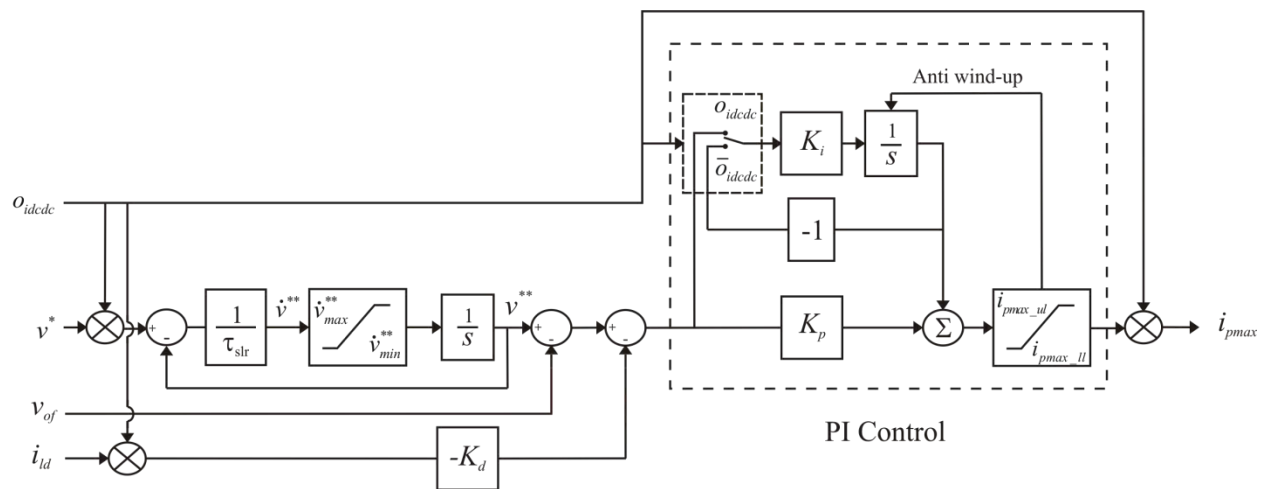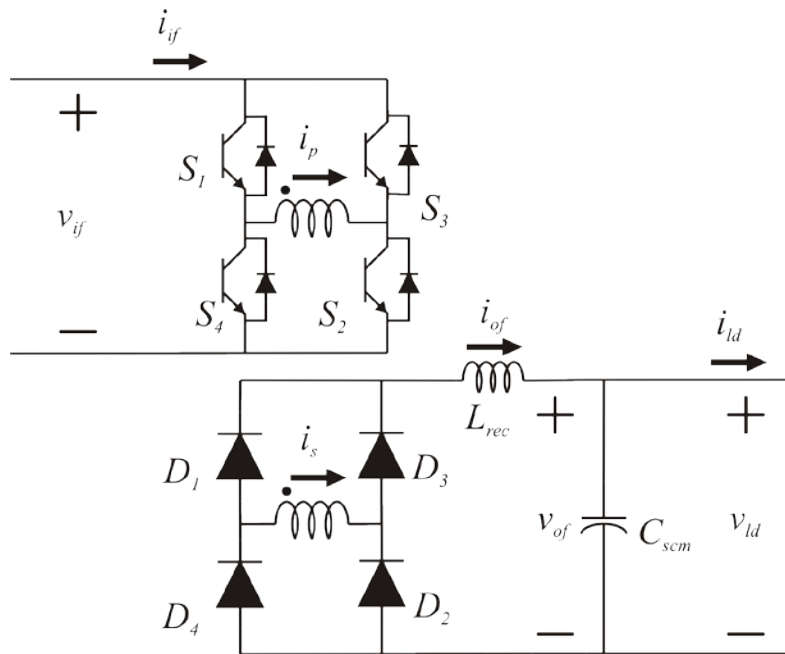**Fig. 5.19.1: DC-DC Converter Topology.**

Fig. 5.19.2: DC-DC Converter Control.

Fig. 5.19.3: AVM Simplified Topology.

The average value model of the IDCDC converter is as follows:

Inputs:

v^* The commanded output filter capacitor voltage (V)

v_{if} The input voltage of the DC-DC converter (V)

i_{ld} The load current drawn from the DC-DC converter (A)

Outputs:

i_{if} The current drawn by the DC-DC converter (A)

v_{of} Output filter capacitor voltage (V)

Parameters:

L_{pcm} Input filter inductance (H)

r_{pcm} Input filter inductor's resistance (Ω)

C_{pcm} Input filter capacitance (F)

L_m Transformer magnetizing inductance (H)

L_{lp} Transformer primary leakage inductance (H)

r_{lp} Transformer primary leakage resistance (Ω)

L_{ls} Transformer secondary leakage inductance (H)

r_{ls} Transformer secondary leakage resistance (Ω)

$\dfrac{N_1}{N_2}$ Transformer turns ratio (no units)

L_{rec} DC link inductance (H)

r_{rec} Resistance of DC link inductor (Ω)

|	
L_{scm}	Output filter inductance (H)
r_{scm}	Output filter inductor's resistance (Ω)
C_{scm}	Output filter capacitance (F)
K_p	Proportional constant (Ω^{-1})
K_i	Integral constant ((Ωs)$^{-1}$)
K_d	Droop constant (Ω)
i_{pmax_ul}	Upper limit of maximum transformer primary current (A)
i_{pmax_ll}	Lower limit of maximum transformer primary current (A)
f_{sw}	Switching frequency of transformer (Hz)
T_{sw}	Time period of switching of transformer (s)
τ_{slr}	Slew rate limit constant (s)
τ_{awu}	Anti-windup constant (s)
$\dot{v}^{**}_{min}$	Minimum rate of change of voltage command (Vs^{-1})
$\dot{v}^{**}_{max}$	Minimum rate of change of voltage command (Vs^{-1})
$v_{in,mns}$	Minimum voltage required at input to enable operation (V)
$v_{in,mxs}$	Maximum voltage allowed at input to enable operation (V)
$v_{in,mnr}$	Minimum voltage required to remain operational (V)
$v_{in,mxr}$	Maximum voltage allowed to remain operational (V)

Interface Equations:
None

States:

v^{**}	The slew-rate limited voltage command (control) (V)
I_{PI}	Integral term in the PI control (A)
v_{of}	Output filter capacitor voltage (V)

Model Equations:

A supervisory control which turns the DC-DC converter on only if the input voltage is within as certain range of voltage and turns the DC-DC converter off if the input voltage is out outside of another range of voltage has also been implemented apart from the main peak-current control. This can be seen in Fig. 5.19.4.
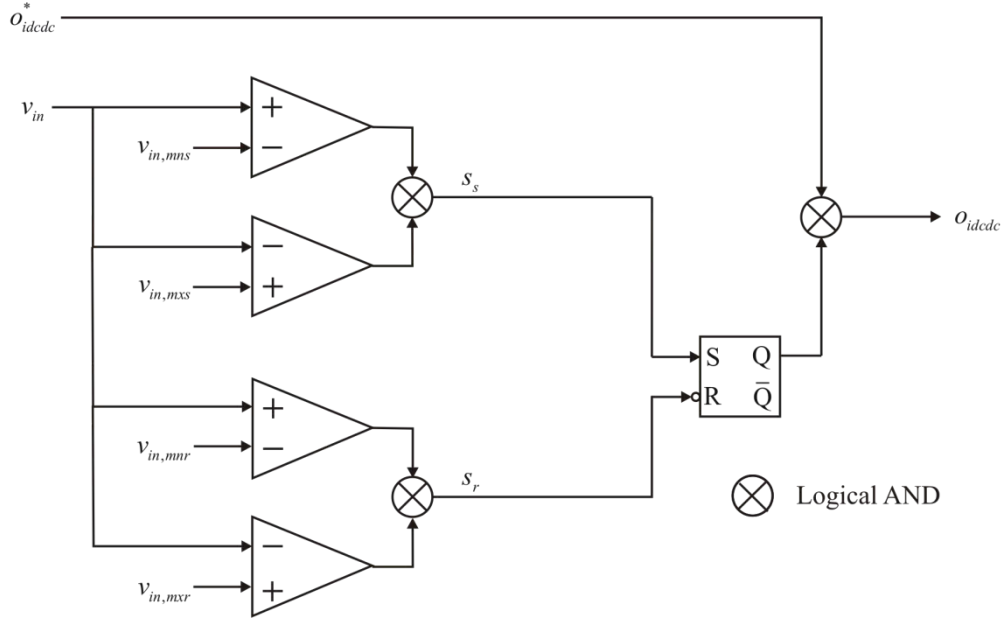
Fig. 5.19.4: Supervisory Control of the DC-DC Converter.

This supervisory control gives as output, o_{idcdc}, which is 1 if the DC-DC converter is operational and 0 if the DC-DC converter is non-operational.

First, the equations that determine the derivative of the states are presented. A variable, $\dot{v}^{**}$ is defined as follows.

$$\dot{v}^{**} = \frac{v^* - v^{**}}{\tau_{slr}} \qquad (5.19.1)$$

where τ_{slr} is the slew-rate limit time constant. The time derivative of the slew-rate limited voltage command is obtained as

$$\frac{d}{dt}v^{**} = \begin{cases} \dot{v}^{**} & \text{if} \quad \dot{v}_{min}^{**} < \dot{v}^{**} < \dot{v}_{max}^{**} \\ \dot{v}_{max}^{**} & \text{if} \quad \dot{v}^{**} > \dot{v}_{max}^{**} \\ \dot{v}_{min}^{**} & \text{if} \quad \dot{v}^{**} < \dot{v}_{min}^{**} \end{cases} \qquad (5.19.2)$$

The PI control with droop is detailed below:

$$v_e = \left(v^{**} - K_d i_{ld}\right)o_{idcdc} - v_{of} \qquad (5.19.3)$$

where k_d is the droop constant and i_{ld} is the load current. The proportional part of the control is obtained as:

$$P_{PI} = K_p v_e \qquad (5.19.4)$$

The integral part of the control is obtained from

$$\frac{d}{dt}I_{PI} = \left(K_i v_e\right)o_{idcdc} + \left(-K_i I_{PI}\right)\overline{o}_{idcdc} + I_{AWU} \qquad (5.19.5)$$

73

$$i_{pmax} = (P_{PI} + I_{PI})o_{idcdc} \qquad (5.19.6)$$

wherein I_{AWU} is anti-windup, which is zero as long as the output of the control, i_{pmax}, is within the prescribed limits. If i_{pmax} is outside the prescribed limits, then the anti-windup can be defined as

$$I_{AWU} = \begin{cases} \dfrac{K_i(i_{pmax\_ul} - i_{pmax})}{\tau_{awu}} & i_{pmax} > i_{pmax\_ul} \\[4mm] \dfrac{K_i(i_{pmax\_ll} - i_{pmax})}{\tau_{awu}} & i_{pmax} < i_{pmax\_ll} \end{cases} \qquad (5.19.7)$$

The time derivative of the output filter capacitor voltage, v_{of} is obtained as

$$\frac{d}{dt}v_{of} = \frac{i_{of} - i_{ld}}{C_{scm}} \qquad (5.19.8)$$

The output filter capacitor voltage, v_{of} is a state and an output. Thus, based on the equations presented above, the only two quantities that need to be derived are i_{of} and i_{if}. These are obtained based on approximating the transformer primary and secondary current waveforms. These are presented in Fig. 5.19.5.
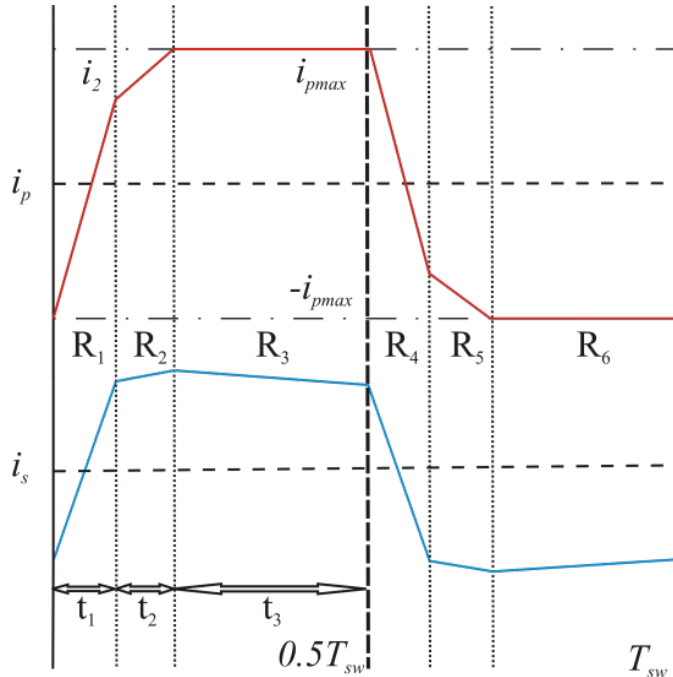

Fig. 5.19.5: Transformer Primary and Secondary Current Waveforms.

The following constants are first described:

$$K = \frac{N_1}{N_2} \tag{5.19.9}$$

$$C_1 = \frac{L_m \left(L_m + L_{ls} + K^2 L_{rec} \right)}{L_m \left(L_{lp} + L_{ls} + K^2 L_{rec} \right) + L_{lp} \left(L_{ls} + K^2 L_{rec} \right)} \tag{5.19.10}$$

$$C_2 = \frac{L_m \left(L_m + L_{lp} \right)}{L_m \left(L_{lp} + L_{ls} + K^2 L_{rec} \right) + L_{lp} \left(L_{ls} + K^2 L_{rec} \right)} \tag{5.19.11}$$

The time in each of the regions: t_1, t_2 and t_3, and i_2 can be obtained as follows:

$$t_1 = \frac{\left(i_2 + i_{pmax} \right)}{v_{if} \dfrac{\left(L_m + L_{ls} \right)}{\left(L_{lp} + L_{ls} \right) L_m + L_{lp} L_{ls}}} \tag{5.19.12}$$

$$t_2 = \frac{\dfrac{v_{of}}{KL_{rec}} \dfrac{Tsw}{2}}{C_2 \left(\dfrac{v_{if}}{L_m + L_{lp}} - \dfrac{Kv_{of}}{L_m} \right) + \dfrac{v_{of}}{KL_{rec}}} \tag{5.19.13}$$

$$t_3 = \frac{T_{sw}}{2} - t_1 - t_2 \tag{5.19.14}$$

where

$$i_2 = i_{pmax} - C_1 t_2 \left(\frac{v_{if}}{L_m} - \frac{Kv_{of}}{L_m + L_{ls} + K^2 L_{rec}} \right) \tag{5.19.15}$$

Using these expressions, i_{of} and i_{if} are obtained as follows:

$$i_{of} = \frac{1}{2} \frac{Kv_{if} L_m t_1}{\left(L_{lp} + L_{ls} \right) L_m + L_{lp} L_{ls}} \tag{5.19.16}$$

$$i_{if} = \frac{\left(\dfrac{-i_{pmax} + i_2}{2} \right) t_1 + \left(\dfrac{i_2 + i_{pmax}}{2} \right) t_2}{\dfrac{T_{sw}}{2}} \tag{5.19.17}$$

Thus, the complete model has been defined.

Validation:

This model is a highly simplified version of the model set forth in [5.21.1]. Although some studies using the model have been compared to detailed waveform level models, and these comparisons have been generally favorable, the model must be viewed as relatively immature.

References:
[5.21.1] Suryanarayana, H.; Sudhoff, S.D., "Average-value modeling of a peak-current controlled galvanically-isolated DC-DC converter for shipboard power distribution," Electric Ship Technologies Symposium (ESTS), 2013 IEEE , vol., no., pp.152,161, 22-24 April 2013.

5.20 DC Fault Detection Unit

The dc fault detection unit consists of a low voltage dc source connected to the DC bus. The unit is depicted in Fig. 5.20.1. This source is used to detect if a fault on the dc bus has been cleared such that the system can be brought back online.
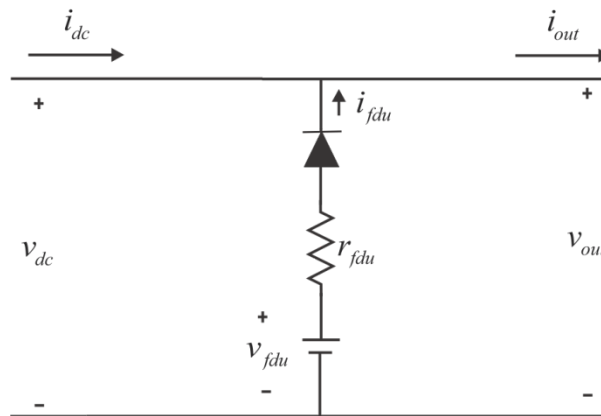
Fig. 5.20.1: DC Fault Detection Unit.

During non-fault operation, there is no current sourced from the fault detection supply due to the series diode. When a fault occurs, the dc voltage of the bus collapses due to fault detection features of the dc bus source. The dc bus will stay at zero as long as the fault is present. Once the fault is cleared, the bus voltage will rise above a threshold defined by the fault detection unit supply voltage. This is an indication to the system that the fault has been cleared and the system can be brought back online. The model structure for the fault detection unit is as follows.

Inputs:

v_{dc} The dc voltage on the bus prior to the unit (V)

i_{out} The dc current on the bus after the unit (A)

Outputs:

v_{out} The dc voltage on the bus after the unit (V)

i_{dc} The dc current in the bus prior to the unit (A)

F The fault status of the system

Parameters:

v_{fdu} The voltage level of the unit (V)

r_{fdu} The resistance of the unit (Ω)

Interface Equations:

$$i_{fdu} = \begin{cases} 0 & v_{dc} \geq v_{fdu} \\ \dfrac{v_{fdu} - v_{dc}}{r_{fdu}} & v_{dc} < v_{fdu} \end{cases}$$ (5.20.1)

$$i_{dc} = i_{out} - i_{fdu}$$ (5.20.2)

States:
None

Model Equations:

The fault status is determined by the voltage level of the bus. If the bus voltage, v_{out}, is less than the voltage level of the detection unit, then there is a fault on the system as the unit is unable to raise the bus voltage above the threshold. Therefore,

$$F = \begin{cases} 0 & v_{out} >= v_{fdu} \\ 1 & v_{out} < v_{fdu} \end{cases}$$ (5.20.3)
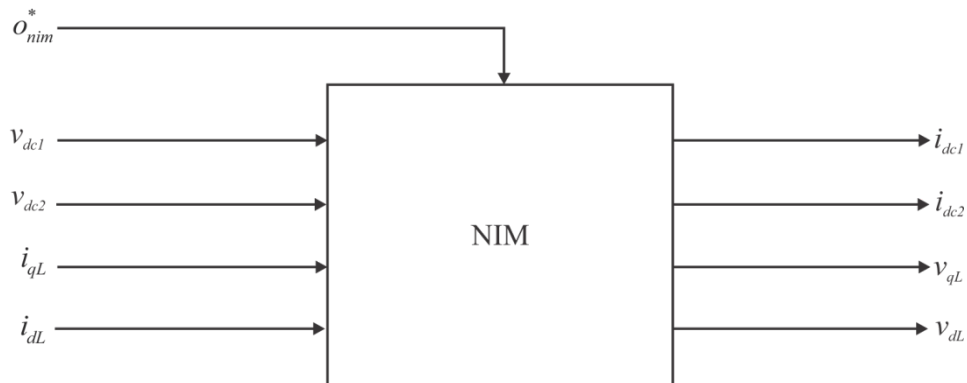
Validation:

This component could certainly be used and implemented in a power system, if desired.

References:
None

5.21 Non-Isolated Inverter Module

The Non-Isolated Inverter Module model is depicted in Fig. 5.21.1.

Fig. 5.21.1: Non-Isolated Inverter Module.

The component model structure is as follows.

Inputs:

v_{dc1} The dc voltage of the primary bus (V)

v_{dc2} The dc voltage of the secondary bus (V)

i_{qL} The q-axis load current (A)

i_{dL} The d-axis load current (A)

o_{nim}^{*} The desired operational status of the component

Outputs:

i_{dc1} The dc current drawn from the primary bus (A)

i_{dc2} The dc current drawn from the secondary bus (A)

v_{qL} The q-axis voltage on the load side (V)

i_{dc2} The d-axis voltage on the load side (V)

P_{out} The output power of the component (W)

Parameters:

i_{Lt} The threshold level load current (A)

i_{Lf} The fault level load current (A)

C The capacitance of the dc bus (F)

τ The time constant associated with the bus capacitance (s)

v_{q}^{*} The desired q-axis output voltage (V)

ω_{e} The electrical speed of the synchronous reference frame (rad/s)

v_{LL}^{*} The desired line-line output voltage (V)

Interface Equations:
None

States:

v_{q} The q-axis output voltage (V)

v_{d} The d-axis output voltage (V)

Model Equations:

    The supervisory control for the NIM is depicted in Fig. 5.21.2. The inputs to the supervisory control are the measured dc voltages on each of the two busses, v_{dc1} and v_{dc2}, and the desired operational status of the load, o_{nim}^{*}.
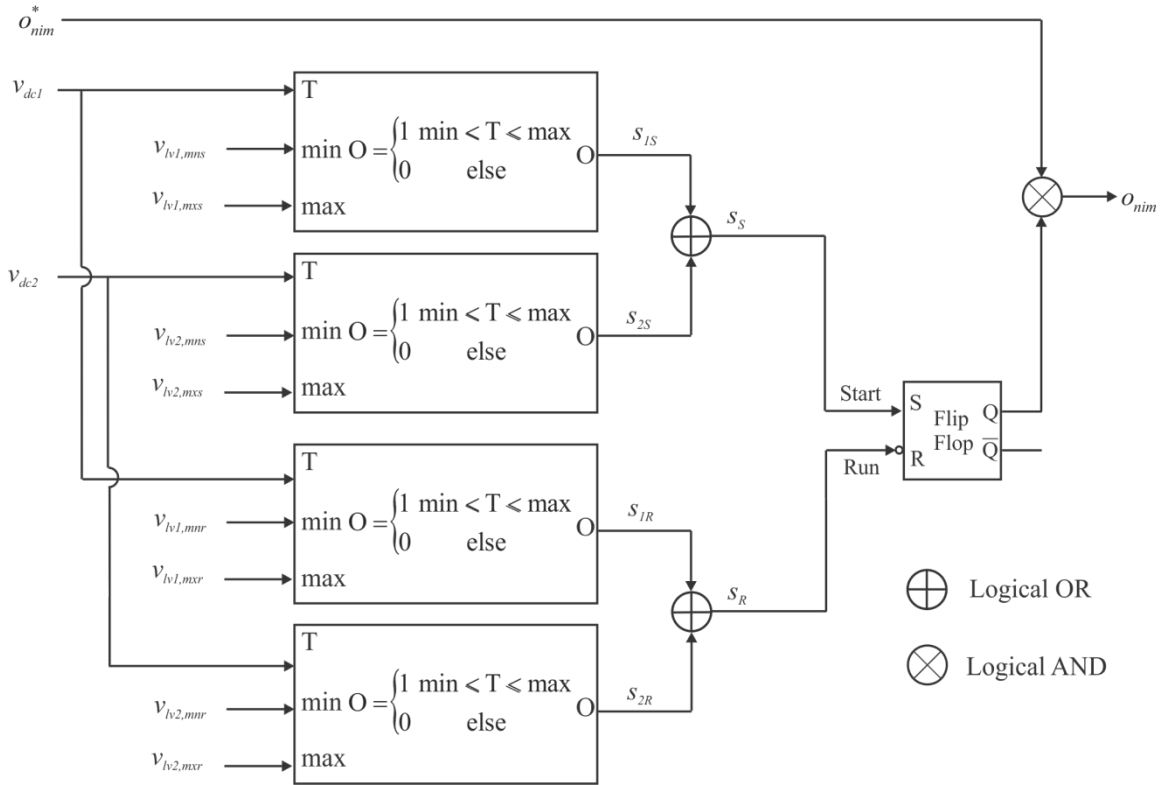
Fig. 5.21.2: NIM Supervisory Control.

The supervisory control categorizes each bus voltage into two categories. The first category relates to being appropriate to start and the second relates to whether the bus voltages are appropriate to continue running. These two conditions have different minimum and maximum voltages level requirements with the startup condition being the more stringent of the two. The output of the control is the operational state of the load, o^*_{nim}, and is dependent upon the voltage levels for each of the busses being within the limits for either the startup or running condition. The intermediate control variables s_{1S} and s_{2S} are true if the corresponding bus voltages are within their ranges governed by the appropriate min and max voltage levels for component start. One bus being within the required range makes the set input of the flip-flop to true. The intermediate control variables s_{1R} and s_{1R} are true if the corresponding bus voltages are within the range governed by the appropriate min and max voltage levels to run. If either of the two busses is within its required voltage range then the flip-flop is not reset. If they both are out of range then the flip-flop is reset.

The first step in calculating the outputs and states for the NIM is to obtain the rms load ac current. Given that the module is in operation, (o=1), this is done using

$$i_{Lrms} = \frac{1}{\sqrt{2}} \sqrt{i_{qL}^2 + i_{dL}^2} \tag{5.20.4}$$

where i_{qL} is the q-axis load current and i_{dL} is the d-axis load current. The desired q-axis output voltage can then be expressed using the relationship depicted in Fig. 5.21.3.
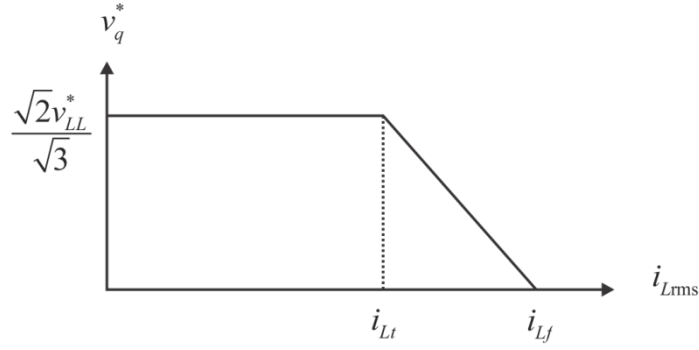
Fig. 5.21.3: NIM *q*-axis Voltage.

In the above figure, the desired *q*-axis voltage is a constant determined by the desired line-line voltage until the rms load current reaches a threshold value where it ramps to zero before the load current can reach the fault threshold. The desired *d*-axis voltage is zero.

Once the desired *q*-axis voltage is determined, the raw *q* and *d* axis currents are calculated using

$$i_{qir} = i_{qL} + \omega_e C v_d + \frac{C}{\tau}\left(v_q^* - v_q\right)$$
(5.20.5)

and

$$i_{dir} = i_{dL} - \omega_e C v_q - \frac{C}{\tau}\left(v_d\right)$$
(5.20.6)

where v_q and v_d are the states of the NIM. The rms raw inverter current is then calculated as

$$i_{mir} = \frac{1}{\sqrt{2}}\sqrt{i_{qir}^2 + i_{dir}^2}$$
(5.20.7)

If the raw rms inverter current, i_{mir}, is less than the threshold load current, i_{Lt}, then

$$i_{qi} = i_{qir}$$
(5.20.8)

and

$$i_{di} = i_{dir}$$
(5.20.9)

Otherwise,

$$i_{qi} = i_{qir}\left(\frac{i_{mir}}{\sqrt{2}i_{Lf}}\right)$$
(5.20.10)

and

$$i_{di} = i_{dir}\left(\frac{i_{mir}}{\sqrt{2}i_{Lf}}\right)$$
(5.20.11)

80

The states of the NIM are obtained from

$$\frac{dv_q}{dt} = \frac{1}{C}\left[i_{qi} - i_{qL} - \omega_e C v_d\right]$$

(5.20.12)

and

$$\frac{dv_d}{dt} = \frac{1}{C}\left[i_{di} - i_{dL} + \omega_e C v_q\right]$$

(5.20.13)

The output power is obtained from

$$P_{out} = \frac{3}{2}\left(v_q i_{qi} + v_d i_{di}\right)$$

(5.20.14)

and the dc current drawn by the NIM from the bus is

$$i_{dc1} = \begin{cases} 0 & o_{nim} = 0 \text{ or } s_{1R} = 0 \\ \dfrac{P_{out}}{v_{dc1}} & o_{nim} = 1 \text{ and } s_{1R} = 1 \end{cases}$$

(5.20.15)

$$i_{dc2} = \begin{cases} 0 & o_{nim} = 0 \text{ or } s_{2R} = 0 \\ \dfrac{P_{out}}{v_{dc2}} & o_{nim} = 1 \text{ and } s_{2R} = 1 \end{cases}$$

(5.20.16)

Validation:

This is a very simple model of the desired behavior of an inverter module. The degree to which it holds is a function of the specific converter design.

References:
None